Reorganization of surviving mammal communities after the end-Pleistocene megafaunal extinction

Authors: Anikó B. Tóth[1]*, S. Kathleen Lyons[2], W. Andrew Barr[3], Anna K. Behrensmeyer[4], Jessica L. Blois[5], René Bobe[6, 7], Matt Davis[8], Andrew Du[9], Jussi T. Eronen[10, 11], J. Tyler Faith[12], Danielle Fraser[13], Nicholas J. Gotelli[14], Gary R. Graves[15, 16], Advait M. Jukar[4], Joshua H. Miller[17], Silvia Pineda-Munoz[4, 18], Laura C. Soul[4], Amelia Villaseñor[19], and John Alroy[1]

Affiliations:

[1]Department of Biological Sciences, Macquarie University, New South Wales 2109, Australia

[2]School of Biological Sciences, University of Nebraska-Lincoln, Lincoln, Nebraska 68588, USA

[3]Center for the Advanced Study of Human Paleobiology, Department of Anthropology, The George Washington University. Washington, D.C. 20052, USA

[4]Department of Paleobiology, Evolution of Terrestrial Ecosystems Program, National Museum of Natural History, Smithsonian Institution, Washington D.C. 20013, USA

[5]School of Natural Sciences, University of California, Merced, 5200 North Lake Road, Merced, California 95343, USA

[6]Departamento de Antropología, Facultad de Ciencias Sociales, Universidad de Chile, Santiago, Chile

[7]Interdisciplinary Center for Archaeology and Evolution of Human Behavior (ICArEHB), Universidade do Algarve, Faro, Portugal

[8]Natural History Museum of Los Angeles Country, 900 Exposition Boulevard, Los Angeles, CA 90007

[9]Department of Organismal Biology and Anatomy, The University of Chicago, 1027 E 57th St., Chicago, IL, 60637, USA.

[10]Ecosystems and Environment Research Programme & Helsinki Institute of Sustainability Science (HELSUS), Faculty of Biological and Environmental Sciences, P.O. Box 65 (Viikinkaari 1), 00014 University of Helsinki, Finland

[11]BIOS Research Unit, Meritullintori 6, 00170 Helsinki, Finland

[12]Natural History Museum of Utah & Department of Anthropology, University of Utah, Salt Lake City UT 84108, USA

[13]Palaeobiology, Canadian Museum of Nature, PO Box 3443 Stn "D", Ottawa ON K1P 6P, Canada

[14]Department of Biology, University of Vermont, Burlington, Vermont 05405, USA

[15]Center for Macroecology, Evolution and Climate, University of Copenhagen, 2100 Copenhagen Ø, Denmark

[16]Department of Vertebrate Zoology, MRC-116, National Museum of Natural History, Smithsonian Institution, PO Box 37012, Washington, D.C. 20013, USA

[17]Department of Geology, University of Cincinnati, Cincinnati, Ohio 45221, USA

[18]Spatial Ecology & Paleontology Lab (SEPL), School of Biological Sciences, Georgia Institute of Technology, Atlanta, Georgia.
[19]Department of Anthropology, University of Arkansas, Fayetteville, Arkansas, 72701, USA

*Correspondence to: aniko.toth@mq.edu.au

Abstract: Large mammals are at high risk of extinction globally. To understand the consequences of their demise for community assembly, we tracked community structure through the end-Pleistocene megafaunal extinction in North America. We decomposed the effects of biotic and abiotic factors by analyzing co-occurrence within the mutual ranges of species pairs. Although shifting climate drove an increase in niche overlap, co-occurrence decreased, signaling shifts in biotic interactions. Furthermore, the effect of abiotic factors on co-occurrence remained constant over time, while the effect of biotic factors decreased. Biotic factors apparently played a key role in continental-scale community assembly before the extinctions. Specifically, large mammals likely promoted co-occurrence in the Pleistocene, and their loss contributed to the modern assembly pattern in which co-occurrence frequently falls below random expectations.
One Sentence Summary: The end-Pleistocene extinction restructured communities of surviving mammals through reduced biotic interactions.

Main Text: Human activities have put extant large-bodied mammals at high risk of extinction (*1*), and their eventual loss may have severe ecological repercussions. For example, the loss of ecosystem engineers such as megaherbivores has the capacity to alter entire landscapes (*2–4*). Such human-mediated extinctions will have impacts lasting far beyond our lifetimes, making it important to examine long-term records of past extinctions to forecast the consequences of current biodiversity loss. A key example is the catastrophic and approximately synchronous (*5*) extinction of large mammals, including mammoths and saber-toothed cats, at the end of the Late

Pleistocene in North America (*6*). The rich and highly resolved Pleistocene and Holocene fossil record provides a unique opportunity to explore how extinction alters communities.

The causes of Pleistocene extinctions have been debated for decades (*7*, *8*). In light of the current biodiversity crisis, recent work has focused on understanding their ecological and evolutionary legacies instead (*9*). A compelling picture of ecological transformation across the continents has emerged, including the disappearance of the mammoth steppe (*2*), changes in vegetation and fire regimes (*10*, *11*), loss of functional groups (*12*), rearrangement of interactions (*13*, *14*), and shifts in global biogeochemistry (*15*) and biophysical feedback systems (*16*). However, empirical studies of changes in mammal community structure, including the extinction of most species over 40 kg (*8*), have often been centered on individual fossil deposits (*17*) or particular taxa (e.g. (*18*, *19*) but see (*20*)).

Here we examine community assembly patterns of surviving large mammals across the Pleistocene-Holocene transition using occupancy, niche size, and patterns of species co-occurrence. We examined end-Pleistocene (21-11 ka), Holocene (11-2 ka), and Recent (2-0 ka) (*21*) mammal occurrence data (Fig. S1) drawn from the FAUNMAP II database (*22*), comprising 93 species (> 1 kg). Only survivor-survivor pairs were analyzed to ensure that community changes were not simply a result of reduced diversity or lost associations involving extinct species. Every possible species pair received an association weight that quantifies how strongly the two co-occur. We refer to a species pair as aggregated when the species occur together more often than expected by chance, and segregated when they co-occur less often than expected. Segregations receive negative weights. Broad shifts in community assembly may be influenced by both extinction and climate change. We estimate the contributions of these two factors by

isolating the relative effects of abiotic and biotic changes on the association of each survivor-survivor pair across this interval.

Species associations are caused by a combination of abiotic and biotic drivers, which can be differentiated by first establishing species' geographic and environmental constraints. Geographic envelopes were constructed using Lambert azimuthal equal area projected coordinates. The climatic envelope of each species was calculated from mean annual temperature, precipitation, temperature seasonality and precipitation seasonality of sites falling within the species' geographic envelopes. Climate estimates were extracted from downscaled paleoclimate simulations (*23*, *24*) and z-transformed. All envelopes were calculated with Blonder's hypervolumes (*25*). The set of sites falling within both geographic and climatic envelopes (Fig. S2) was defined as the potential range of each species. The potential range represents sites where the occurrence of a species is not constrained by climate or dispersal ability. We also calculated background climatic and geographic hypervolumes for each species in each time interval to quantify how much of the available geographic and environmental space is being occupied by each species (*21*).

We calculated the strength and direction of pairwise co-occurrence of species pairs with the mid-P variant of Fisher's Exact Test, which provides an association weight for each pair (*26*). We then individually calculated biotic and abiotic components of co-occurrence, such that the sum of the association weights of these two components equals the original association weight (Fig. S3). We did this by calculating the association weight within the mutual potential range (i.e., the sites remaining after accounting for abiotic limits for both species), which represents the component of each association regulated by biotic factors. The abiotic component was defined as the difference between the full association and its biotic component (*21*). The abiotic component

of a pair received a positive association weight if species have similar niches, and negative if their niches were disparate (Fig. S3). The biotic and abiotic components of a pair may have the same or opposite signs, and when the latter occurs the full association weight may be close to 0 (Fig. S3). Using this framework, we evaluated changes in co-occurrence patterns and their components across the Pleistocene-Holocene transition and into the Recent.

Across the Pleistocene-Holocene transition, common surviving species became even more common and rare species remained the same or became rarer (Fig. 1A). There were no significant changes in occupancy patterns between the Holocene and the Recent (Fig. 1B). Extinction victims had smaller climatic and geographic envelopes than survivors in the end-Pleistocene (Fig. 2). On average, climatic and geographic envelopes of surviving species expanded from the end-Pleistocene to the Holocene, even when compared to background variation (i.e., as a proportion of the total space each species could potentially occupy; Fig. 2).

Aggregations were dominant for survivor pairs in the end-Pleistocene, and segregations increased in the Holocene and Recent (Fig. 3E-F). There was also a marked decrease in association weights for aggregations and an increase for segregations over the Pleistocene-Holocene transition (Fig. 3K-L). We considered and ruled out several confounding factors such as sampling and dating biases (*21*). Observed occupancy changes between the time intervals predict stronger associations and increased proportion of aggregations (*21*). While this may partially explain why segregations became stronger, it cannot explain the increase in proportion of segregations or the decrease in aggregation strengths. When associations were split into their biotic and abiotic components, end-Pleistocene associations calculated within mutual potential ranges of pairs (i.e., biotic associations) were also dominated by aggregations, which diminished in both mean weight (Fig. 3I) and as a proportion of the pairs (Fig. 3C) across the Pleistocene-

Holocene transition, while segregations increased in mean weight and proportionally (Figs. 3J and 3D). Abiotic associations (i.e., the difference between the full association and the biotic association) exhibited the opposite pattern (Figs. 3A-B, G-H). Note that associations due to abiotic components were typically segregations while those due to biotic components were typically aggregations, and this pattern was greatly weakened but not overturned by the trends described above.

The Pleistocene-Holocene transition was characterized by substantial changes in occupancy (Fig. 1), niche size (Fig. 2), and association patterns (Fig 3). The fact that survivors of the extinction exhibited larger potential ranges than the victims (Fig. 2) is consistent with the concept that specialists with narrow ranges are at higher risk of extinction (*1*). The expansion of climatic niche fill in the Holocene may reflect the filling of empty niche space after competitive release.

The overall shift toward segregations starting in the Holocene resulted from changes in the relative effects of the biotic and abiotic components of species co-occurrence. Increasing climatic and geographic niche fill (Fig. 2E) drives increasing potential range overlap between pairs in the Holocene (Fig. S4), and this caused the shift toward aggregations in abiotic associations. In contrast, co-occurrence decreased within mutual potential ranges (i.e., biotic associations; Fig. 3C-D). All else being equal, these opposing forces might have nullified any trend in the full associations. We observe a trend, however, because of the change in the relative importance of biotic and abiotic factors, which can be quantified using the average magnitude (absolute value) of association weights within each component. Species responses to environmental factors contributed consistently to community assembly over time despite the dramatic climatic changes driving species dispersal over this interval (*27*), while co-occurrence

patterns due to biotic interactions diminished after the end-Pleistocene (Fig. 4). The loss of biotic associations increases segregations, because biotic interactions tend to promote aggregations. Thus, the decrease in co-occurrence was driven by the combined effects of weakening biotic associations and a decrease in the tendency of biotic associations to be aggregated. Therefore, shifting biotic factors (i.e. the loss of the megafauna or the advent of humans), not climate change, were responsible for the ecological upheaval.

It is difficult to determine from our results whether the change in survivor co-occurrence is a direct result of the loss of survivor-victim interactions, more indirectly due to the loss of megafauna in their role as ecosystem engineers, or other contemporaneous changes such as increasing human impacts. Pleistocene predators were often more specialized (*28*), and their loss may have allowed survivors to consume a wider range of prey species, reducing the need to co-occur strongly with primary prey species and weakening aggregations. In addition, the loss of large-bodied prey could have caused prey-shifting to more abundant smaller-bodied mammals and thus reduced fidelity to any particular prey species (*18*). Segregations also increased in abundance and magnitude within mutual potential ranges. One potential explanation is that the loss of predators and competitors increased the abundances of survivors in a rapid competitive release scenario (*29*) that eventually led to enhanced competition and increased exclusion.

Contemporary loss of keystone species causes direct and indirect effects on other species and communities (*4*, *30*, *31*) via the loss of biotic interactions. These include top-down biotic processes (*4*), higher-order interactions (i.e., a third species affecting the interaction of two others) (*32*), ecosystem engineering, pest control, and nutrient cycling (*16*). Such loss often results in reduced biodiversity and degradation of ecosystem health. The extinction of the megafauna may have caused substantial shifts in the biotic drivers of community assembly via

similar pathways, particularly via the loss of top-down control and the liberation of resources. The trend away from aggregations is crucial because it has been suggested that coexistence enhances biodiversity through the emergence of higher-order interactions (*32*), and biodiversity is a central focus of modern conservation efforts.

The end-Pleistocene extinction caused measurable, lasting effects on the dynamics of mammal communities that went beyond simple biodiversity loss. Our analysis suggests that these losses disrupted a network of species interactions that supported high levels of aggregation, leading to a modern fauna in which continent-wide species associations are now regulated more strongly by climate and dispersal limitation and are characterized increasingly by segregation. We find that biotic mechanisms such as species interactions and range dynamics once played a measurable role in mammal community assembly by consistently affecting how species co-occurred on continental scales. Remaining species interactions among survivors likely take place opportunistically, on smaller scales, or within shorter timeframes. Overall, we find that biotic mechanisms now play a reduced role in species co-occurrences on a continental spatial scale, and this shift was most likely driven by the extinction of the Pleistocene megafauna.

References and Notes:

1. A. D. Davidson, M. J. Hamilton, A. G. Boyer, J. H. Brown, G. Ceballos, *Proc. Natl. Acad. Sci. U. S. A.* **106**, 10702–10705 (2009).

2. S. A. Zimov *et al.*, *Am. Nat.* **146**, 765–794 (1995).

3. W. J. Ripple *et al.*, *Bioscience*. **66**, 807–812 (2016).

4. J. A. Estes *et al.*, *Science.* **333**, 301–306 (2011).

5. J. T. Faith, T. A. Surovell, *Proc. Natl. Acad. Sci. U. S. A.* **106**, 20641–5 (2009).

6. A. D. Barnosky *et al.*, *Science.* **355**, 4787 (2017).

7. P. L. Koch, A. D. Barnosky, *Annu. Rev. Ecol. Evol. Syst*. **37**, 215–250 (2006).

8. S. K. Lyons, F. A. Smith, J. H. Brown, *Evol. Ecol. Res.* **6**, 339–358 (2004).

9. Y. Malhi *et al.*, *PNAS*. **113**, 838–846 (2016).

10. J. L. Gill, J. W. Williams, S. T. Jackson, K. B. Lininger, G. S. Robinson, *Science.* **326**, 1100–1103 (2009).

11. S. Rule *et al.*, *Science.* **335**, 1483–1486 (2012).

12. M. Davis, *Proc. R. Soc. London B Biol. Sci.* **284**, 1–7 (2017).

13. M. Galetti *et al.*, *Biol. Rev.* (2017), doi:10.1111/brv.12374.

14. S. K. Lyons *et al.*, *Nature*. **529**, 80–83 (2016).

15. F. A. Smith *et al.*, *Proc. Natl. Acad. Sci. U. S. A.* **113**, 874–879 (2016).

16. C. E. Doughty *et al.*, *Proc. Natl. Acad. Sci. U. S. A.* **113**, 868–73 (2016).

17. F. A. Smith *et al.*, *Ecography (Cop.).* **39**, 223–239 (2016).

18. M. W. Hayward *et al.*, *Front. Ecol. Evol.* **3**, 148 (2016).

19. M. I. Pardi, F. A. Smith, *Ecography (Cop.).* **39**, 141–151 (2016).

20. S. K. Lyons, *Am. Nat.* **165**, E168-85 (2005).

21. Materials and methods are available as supplementary materials at the Science website.

22. R. W. Graham, E. L. Lundelius, *FAUNMAP II Database, version 1.0* (2010) (available at http://www.ucmp.berkeley.edu/neomap/use.html).

23. Z. Liu *et al.*, *Science.* **325**, 310–314 (2009).

24. S. D. Veloz *et al.*, *Glob. Chang. Biol.* **18**, 1698–1713 (2012).

25. B. Blonder, C. Lamanna, C. Violle, B. J. Enquist, *Glob. Ecol. Biogeogr.* **23**, 595–609 (2014).

26. A. Kallio, K. Puolamäki, M. Fortelius, H. Mannila, *Palaeontol. Electron.* **14** (2011).

27. R. W. Graham *et al.*, *Science.* **272**, 1601–1606 (1996).

28. B. Van Valkenburgh, X. Wang, J. Damuth, *Science.* **306**, 101–104 (2004).

29. J. Alroy, *Science.* **292**, 1893–1896 (2001).

30. R. L. Beschta, W. J. Ripple, *Biol. Conserv.* **142**, 2401–2414 (2009).

31. W. J. Ripple *et al.*, *Sci. Adv.* **1**, e1400103 (2015).

32. J. M. Levine, J. Bascompte, P. B. Adler, S. Allesina, *Nature*. **546**, 56–64 (2017).

33. F. A. Smith *et al.*, *Ecology*. **84**, 3403–3403 (2003).

34. P. J. Reimer *et al.*, *Radiocarbon*. **55**, 1869–1887 (2013).

35. M. Niu, B. T. J Heaton, B. P. G Blackwell, B. C. E Buck, *Radiocarbon*. **55**, 1905–1922 (2013).

36. C. Bronk Ramsey, *Radiocarbon*. **37**, 425–430 (1995).

37. S. S. Hughes, *J. Mammal.* **90**, 74–92 (2009).

38. R. Dale Guthrie, *Nature*. **429**, 746–749 (2004).

39. J. L. Blois, P. L. Zarnetske, M. C. Fitzpatrick, S. Finnegan, *Science.* **341**, 499–504 (2013).

40. M. B. Araújo, M. Luoto, *Glob. Ecol. Biogeogr.* **16**, 743–753 (2007).

41. A. Barberán, S. T. Bates, E. O. Casamayor, N. Fierer, *ISME J.* **6**, 343–351 (2012).

42. P. W. Lane, D. B. Lindenmayer, P. S. Barton, W. Blanchard, M. J. Westgate, *Ecol. Evol.* **4**, 3279–3289 (2014).

43. W. Ulrich, F. Jabot, N. J. Gotelli, *Oikos*. **126**, 91–100 (2017).

44. G. Berry, P. Armitage, *Stat.* **44**, 417–423 (1995).

45. J. A. Veech, *Glob. Ecol. Biogeogr.* **22**, 252–260 (2013).

46. D. J. Harris, *Ecology*. **97**, 3308–3314 (2016).

47. N. J. Gotelli, *Ecology*. **81**, 2606–2621 (2000).

48. E. M. H. and A. M. E. Nicholas J. Gotelli, EcoSimR (2015), (available at https://cran.r-project.org/web/packages/EcoSimR/citation.html).

49. B. G. Jonsson, *Oecologia*. **127**, 309–313 (2001).

50. R. K. Colwell, D. W. Winkler, in *Ecological Communities: Conceptual Issues and the Evidence* , A. B. T. Donald R. Strong, Daniel Simberloff, Lawrence G. Abele, Ed. (Princeton University Press, 1984; https://app.dimensions.ai/details/publication/pub.1011228949), pp. 344–359.

51. M. A. Leibold, G. M. Mikkelson, *Oikos*. **97**, 237–250 (2002).

52. W. A. Burroughs, J. C. Brower, *Comput. Geosci.* **8**, 137–148 (1982).

53. S. J. Presley, C. L. Higgins, C. López-González, R. D. Stevens, *Oecologia*. **160**, 781–793 (2009).

54. P. Andrews, *Owls, caves, and fossils : predation, preservation, and accumulation of small mammal bones in caves, with an analysis of the Pleistocene cave faunas from Westbury-*

sub-Mendip, Somerset, UK (University of Chicago Press, Chicago, 1990).

55. J. H. Brown, *Macroecology* (University of Chicago Press, 1995).

56. R. E. Plotnick, F. A. Smith, S. K. Lyons, *Ecol. Lett.* **19**, 546–553 (2016).

57. G. D. Zazula *et al.*, *PNAS*. **111**, 18460–18465 (2014).

58. G. D. Zazula *et al.*, *Quat. Sci. Rev.* **171**, 48–57 (2017).

Acknowledgments: We thank the Macquarie University paleobiology lab for discussions that improved this paper.

Funding: Support for this research was provided by the Smithsonian Institution's National Museum of Natural History Program grant to the Evolution of Terrestrial Ecosystems Program (ETE) and NSF-DEB 1257625. This is ETE publication #382. ABT was supported by an MQRES scholarship from Macquarie University.

Author contributions: All authors contributed to the development and interpretation of the ideas in this manuscript and edited the manuscript. ABT helped design the study, curated and analyzed data, produced the figures, and wrote the paper. SKL and JA were involved in the study design and draft preparation. SKL, JA, JTF, JHM, JTE, GG, NG, AKB, MD, and AMJ helped design supporting analyses.

Competing Interests: The authors declare no competing interests.

Data and materials availability: All R scripts and cleaned datasets used for this analysis are available at https://github.com/anikobtoth/Megafauna.

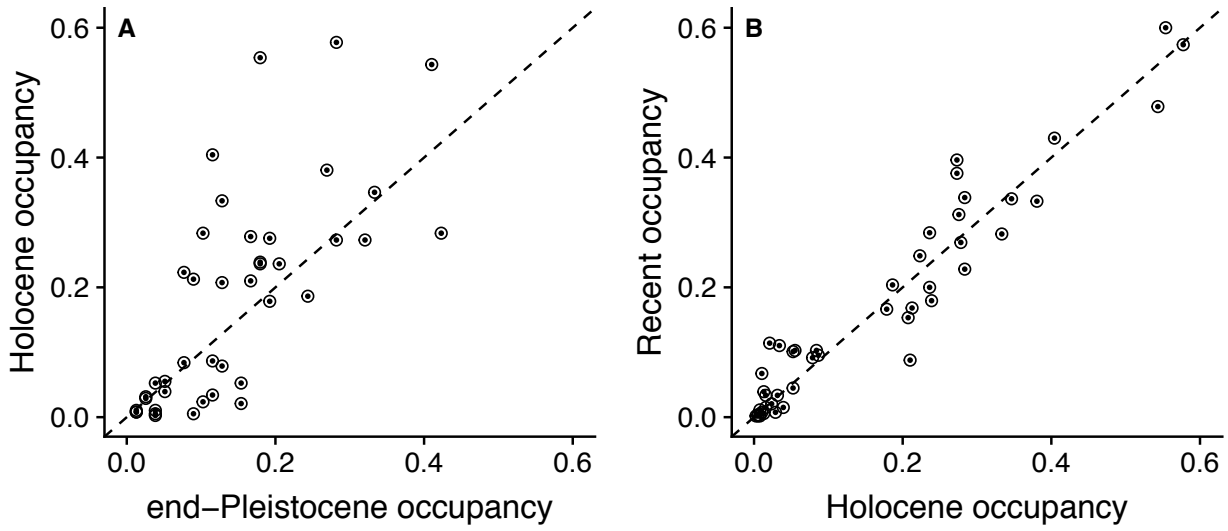

Figure 1. **Comparison of survivor occupancy across time intervals.** (A) End-Pleistocene to Holocene ($N = 44$) and (B) Holocene to Recent ($N = 45$). Points are species. The line of unity is shown.

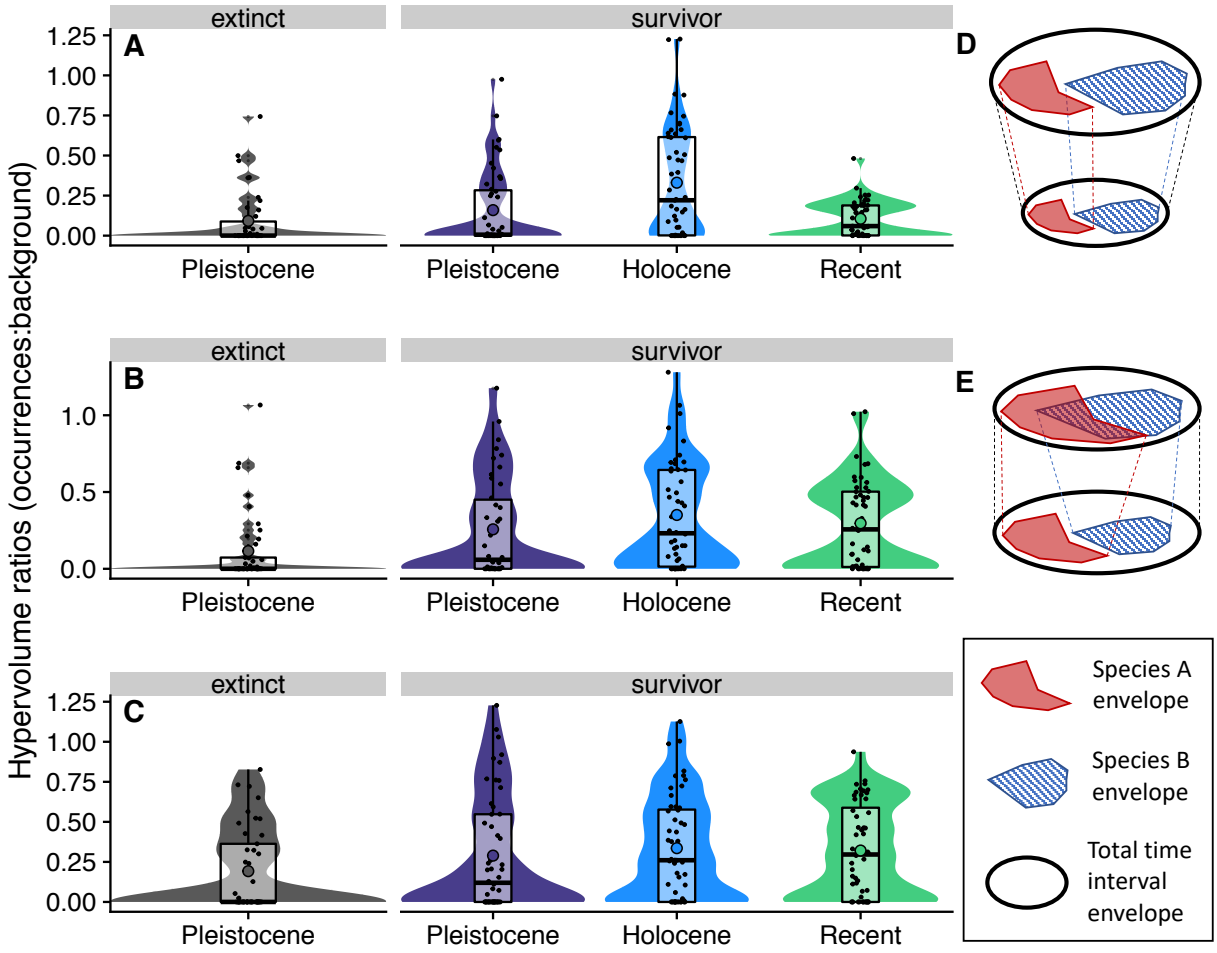

Figure 2. Changes in niche fill. Hypervolume ratios of climatic (A-B) and geographic (C) envelopes of species with respect to the breadth of (A) pooled unoccupied climate envelopes by species, and (B-C) total unoccupied envelopes in each time interval. In (A) larger ratios correspond to expanded envelopes from space available in time intervals (D), and in (B-C) larger ratios correspond to proportionally higher fill that causes increased overlap (E). Shaded distributions represent area of 1, circles are means.

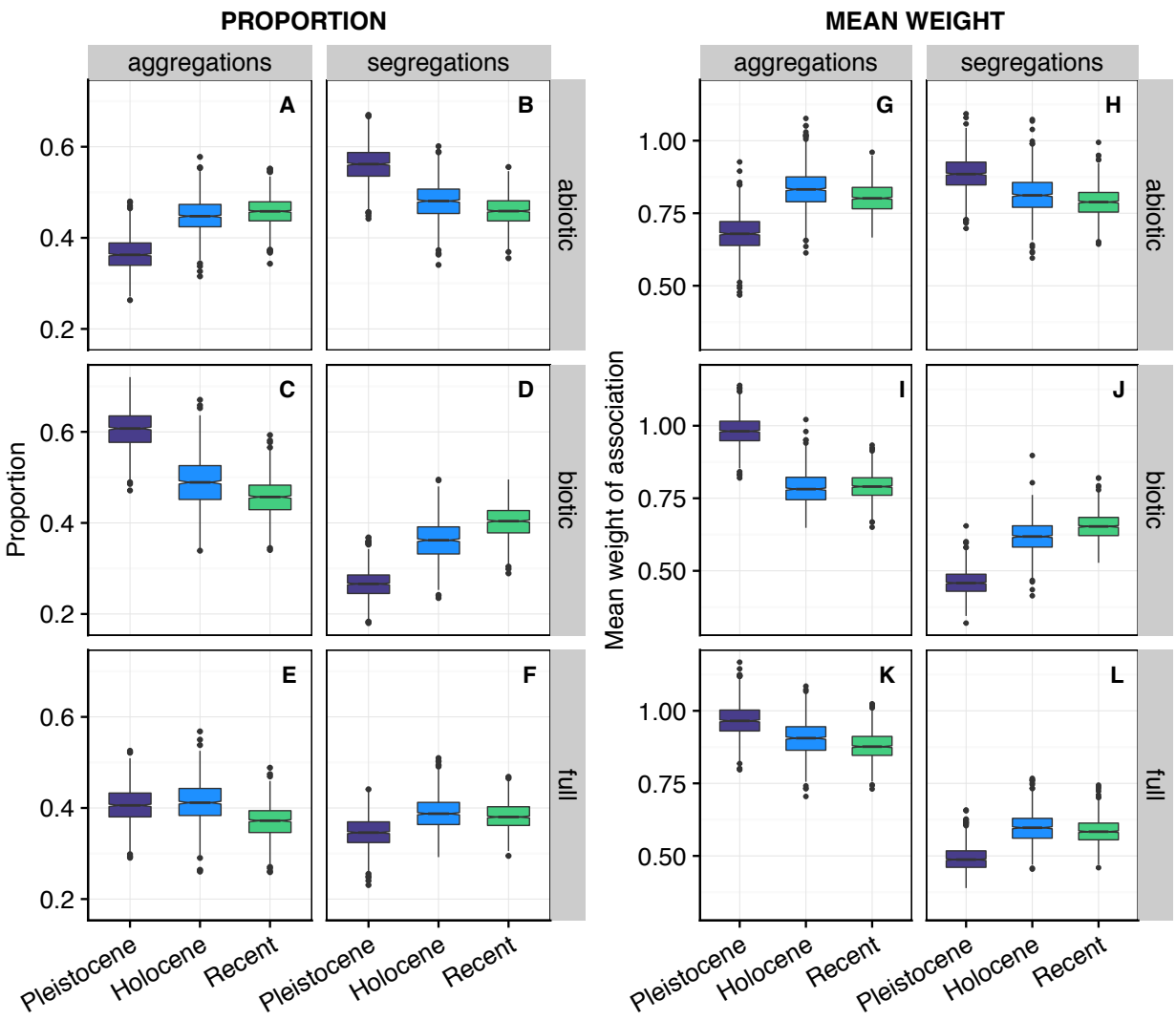

Figure 3. Proportion and mean weight of aggregations and segregations. Proportion (A-F) and mean weight (G-L) of aggregations and segregations for abiotic components (A-B, G-H), biotic components (C-D, I-J), and full associations (E-F, K-L) in each subsample (n = 1000). Excludes associations with weight of 0.

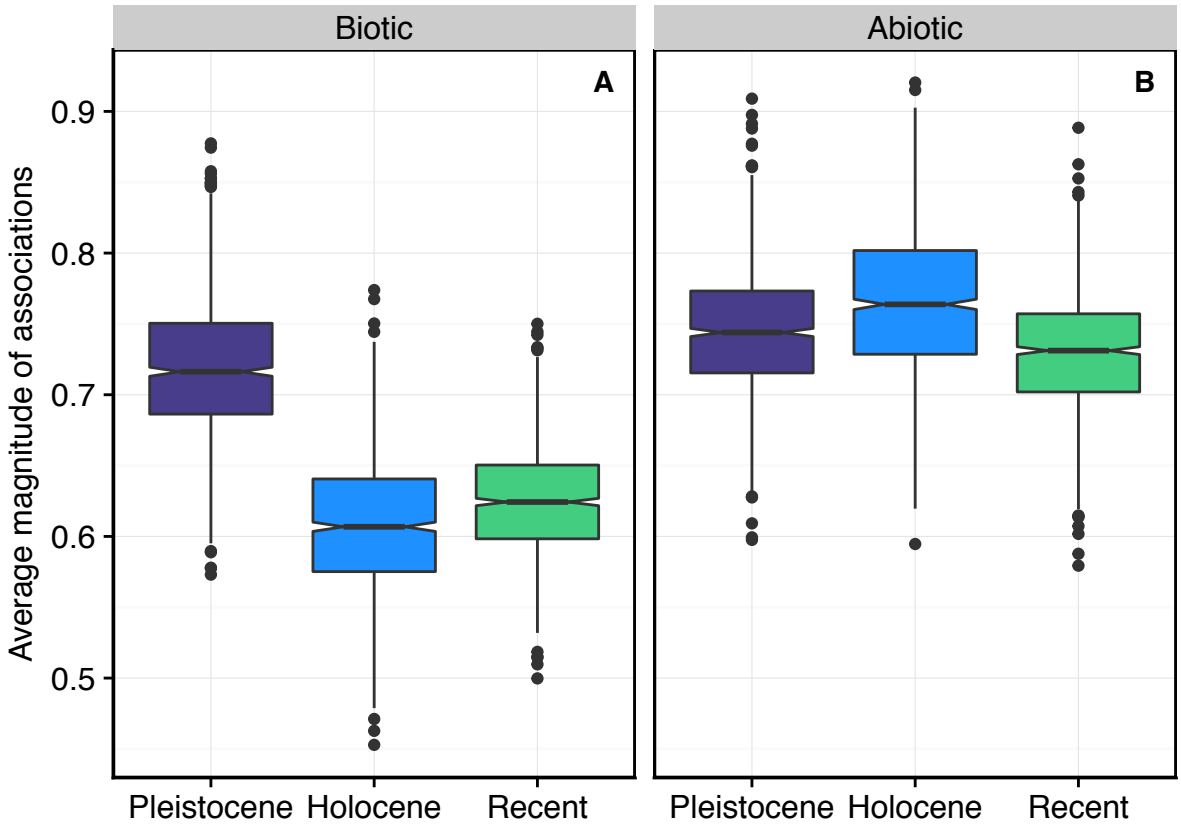

Figure 4. Average magnitude of biotic and abiotic associations. Absolute values of associations weights, broadly representing the relative importance of biotic and abiotic components for overall community assembly patterns. Boxplots represent the variation among subsamples (n = 1000).

Supplementary Materials for

Reorganization of surviving mammalian communities after the end-Pleistocene mass extinction

Anikó B. Tóth, S. Kathleen Lyons, W. Andrew Barr, Anna K. Behrensmeyer, Jessica L. Blois, René Bobe, Matt Davis, Andrew Du, Jussi T. Eronen, J. Tyler Faith, Danielle Fraser, Nicholas J. Gotelli, Gary R. Graves, Advait M. Jukar, Joshua H. Miller, Silvia Pineda-Munoz, Laura C. Soul, Amelia Villaseñor, and John Alroy

correspondence to: aniko.toth@mq.edu.au

This PDF file includes:

Materials and Methods

Data

We obtained species-by-site tables of mammal occurrences from the FAUNMAP II database (*22*), which documents fossil localities across North America (excluding Mexico; Fig. S1). Using the pre-existing FAUNMAP epoch classifications, we extracted sites from the Holocene and Late Pleistocene. A site is defined as an entity having a unique combination of the fields 'analysis unit' and 'machine number', so different strata from the same locality were treated as separate sites (see supplemental section on time averaging for a discussion of the effects of site duration). We did not use sites whose FAUNMAP epoch classifications were not clearly Holocene or Pleistocene. Although dating of individual sites within FAUNMAP is often imprecise, this treatment ensured that the Holocene and Pleistocene species clearly represent pre- and post-extinction faunas (i.e. communities with extinct megafauna and communities without them), despite some minor inconsistencies in dating boundaries. Finally, we removed indeterminate species and marine species such as cetaceans, sirenians, pinnipeds, and sea otters.

We obtained mean body mass estimates for fully identified species from the Body Mass of Late Quaternary Mammals database (*33*), and removed species with mass estimates less than 1 kg, which also excluded bats from the analysis. We did this to focus our main analysis on larger species, but also to avoid biases associated with sampling methods, which differ for small and large mammals. From the resulting species-by-site tables (one for each time interval), we removed sites that were above a latitude of 60˚N in order to avoid artificial biogeographic biases introduced by the large unsampled area separating Alaska and the Yukon from the rest of the sites.

We then discarded sites with fewer than five species to exclude samples which are unlikely to reflect the original communities and to increase the computational speed and accuracy of community analyses. Including a large number of sites with only one or a few species would result in very low matrix fill, and therefore artificially cause co-occurrence results to be biased heavily toward negative associations.

We downloaded the locality data table from FAUNMAP and extracted metadata on our remaining sites. We calibrated all uncalibrated ^{14}C dates with the IntCal13 calibration curve (*34*, *35*) in OxCal (*36*). The dates of sites estimated with other methods were left unchanged. This is unlikely to bias our analyses because the sites were grouped into broad intervals for our analyses, where the most important distinction was the separation of pre- and post-extinction faunas. We left the Pleistocene data in their original FAUNMAP epoch categories, but we divided the Holocene epoch into Holocene and Recent time intervals, setting the boundary at a maximum calendar date of 2 ka. We limited the end-Pleistocene interval to sites whose mean age was younger than 21 ka. This is the oldest interval that has associated climate simulations, and taking this step also accounts for bias associated with time averaging by establishing roughly equal temporal durations for the end-Pleistocene (9.3 ka) and the Holocene time intervals (9.7 ka).

Climates were inferred from the CCSM3 paleoclimate simulations (*23*), which were downscaled to 0.5º x 0.5º at 1000-year intervals from 0 to 21 ka (*24*). We extracted mean annual precipitation and mean annual temperature for each site, matching the mean calibrated calendar ages of sites to the corresponding climate inferences. We excluded sites for which we could not estimate climate (i.e., sites assigned to a single epoch in FAUNMAP but lacking dates).

The final dataset had the following time intervals: end-Pleistocene (21-11 ka), Holocene (11-2 ka), and Recent (2-0 ka). The general properties of our final dataset are listed in Table S1, and their locations are mapped in Fig. S1. The end-Pleistocene dataset includes 83 species, the

Holocene 48 species, and the Recent 48 species (Table S1), and 45 of the latter are sampled in both the Recent and Holocene, for a total of 51 surviving species. The discrepancy between Holocene and Recent data sets is due to less common species not being sampled in both time intervals. Of the end-Pleistocene species, 45 survived and 53 went extinct (i.e., they were not sampled in the Holocene and Recent and are listed as extinct in the recent literature). The only contentious extinction was that of *Martes nobilis,* which was considered an extinct species distinct from *M. americana* in this study (*37*). The taxonomy of extinct mammals does not affect our analysis, as we only compared associations among surviving species. For instance, there is a lack of consensus about the splitting of extinct *Equus* species, but it is widely accepted that only one species, *E. ferus*, is still extant. Finally, it is widely known that some extinct species may have survived briefly into the Holocene (*38*). Because we wished to compare surviving faunas pre- and post-extinction, the sites in our time intervals represent pre- and post-extinction faunas, even at the expense of precise date boundaries. In other words, Holocene-dated sites that include any remnants of megafauna were not included in our Holocene dataset. The dataset represents 105 species in total. With the exception of the niche space analyses, which included a category for extinction victims, the central analyses in this manuscript are focused on community changes of the survivors across the three time intervals. This is because we were interested in how changes over the extinction interval affected the community structure of extant species.

Niche space analysis

Understanding the breadth of the geographic extent and climatic niche of each species helps to interpret how abiotic factors affected the co-occurrence structure of the assemblage pre- and post-extinction. We estimated the climatic and geographic envelopes of each species, and then compared the sizes of these envelopes to several types of backgrounds.

We estimated the realized climatic envelope (*C*) and geographic envelope (*G*) of each species *i* in each time interval in two ways. First, we used Blonder's hypervolume package (*25*) in R to construct a hypervolumes with the geographic coordinates (projected into the Lambert azimuthal equal area projection and z-transformed to make them more comparable to climatic envelopes) of each occurrence of species *i*. These hypervolumes represent the geographic envelope G_i of each species. We repeated the process to make climatic envelopes C_i using z-transformed mean annual precipitation, mean annual temperature, precipitation seasonality, and temperature seasonality, extracted for each site from the temporally corresponding layer in a previously published, downscaled paleoclimate simulation (*23*, *24*). Mean annual precipitation and precipitation seasonality were also square root transformed before calculating z-scores. Climatic envelopes were calculated only from sites falling within the geographic envelope of each species in each time interval. We then compared the sizes of these climate envelopes to three background variations.

First, to investigate changes in the degree of niche infilling over time, we calculated background climate from the absences within each species geographic niche within each time interval (background 1). This comparison explores the extent to which species filled the climatic niche that they accessed in each time interval.

Second, to investigate changes in the degree of potential niche infilling over time, we calculated a background climate from the pooled absences within the geographic envelope of each species across all three time intervals (background 2). This comparison asks: in each time

interval, to what extent did species fill the climatic niche that they accessed over all time intervals? This also addresses the question of whether, objectively, the niches of species expanded or contracted, whether or not the background variability changed. We expect time intervals with larger overall climatic variability to exhibit larger niche sizes.

Third, to investigate changes in the degree of available niche fill over time, we calculated background climate from the absences of each species within each time interval (background 3). This comparison investigates the extent to which species filled the climatic niche that they had the ability to access within each time interval. Mammal species, particularly larger-bodied mammal species, are very mobile and are easily able to disperse thousands of kilometers over time intervals as long as the ones in this study. Environmental and biotic factors, not physical boundaries or physiological limitations, would have constrained their realized geographic envelopes. The purpose of calculating background this way was to understand how much climate space was utilized by each species with respect to the total unused available background, because this influences the degree of overlap in the potential ranges of species, which has bearing on the abiotic component of the co-occurrence analysis.

We did not include geographic and climatic variables in the same hypervolumes because geographic coordinates are often collinear with climatic variables, and this restricts the hypervolumes to a hyperplane, strongly affecting volume calculations. Including collinear variables in the same hypervolume is not recommended by Blonder et al. (*25*). Furthermore, species are not biologically confined to particular combinations of climate and geographic location. Species should disperse to any sites with suitable climatic conditions as long as they are able to reach them.

We repeated this process using simple convex hulls instead of hypervolumes to calculate geographic, climatic, and seasonality envelopes. Geographic range was estimated for each species *i* by calculating the area of the convex hull G_i around the locations (plotted using the Lambert azimuthal equal area projection and z-transformed) where the species occurred. Climatic envelope was estimated by calculating the area of the convex hull C_i around occurrences plotted by their mean annual temperature in ˚C and square root transformed mean annual precipitation in mm/year, taken for each site from the temporally corresponding layer in a previously published, downscaled paleoclimate simulation (*23*, *24*) and z-transformed. Seasonality envelope was estimated by taking the area of the convex hull S_i around the occurrences of each species plotted by z-transformed temperature and precipitation seasonality (from the same source as mean annual climate data).

We compared estimated geographic envelope and climate envelope areas for victims of the extinction in the end-Pleistocene and survivors across the three time intervals. In the main text, we present the areas of the hypervolume-based geographic envelopes with respect to unoccupied geographic space, and the volumes of climatic envelopes with respect to backgrounds 2 and 3 described above (Fig. 2). We present the raw hypervolume sizes and background 1 in Fig. S5. All of the convex hull results (including raw areas and areas with respect to background variation) are presented in Figs. S6-7.

The potential range of each species was then calculated as the intersection of the climate and geographic envelopes for that species across the entire time interval (Fig. S2). The set of sites in the potential range of each species (P_i) thus consists of all the sites where the species occurred, plus any additional sites that fall within both G_i and C_i, thereby ensuring that they are environmentally suitable and geographically accessible for species *i*. The collection of sites within the potential ranges of species were used later to conduct the analysis of mutual potential

range co-occurrence. Potential ranges based on hypervolumes are used in the main text, but the same analyses using convex hulls are included in the supplementary figures.

Co-occurrence analysis

Interactions between species are recognized as crucial to community assembly (*39*). Co-occurrence analysis quantifies the association between species pairs based on the frequency with which they are found at the same sites, and has increasingly been used to characterize the structure and dynamics of communities (*14*, *40–43*). To remove the confounding effect of sample size, we subsampled (without replacement) the species-by-site occurrence matrices (one each for end-Pleistocene, Holocene, and Recent) to 60 sites, computed pairwise Fisher's Exact Test mid-P variant co-occurrence scores, or weights, (*26*, *44*) for all possible pairs in each subsample, and repeated this process 1000 times. Note that the null model for this analysis is included in the calculation of the mid-P variant of Fisher's Exact test, described in the next paragraph. The random subsampling procedure was used to standardize sample size across the time intervals, not to build a null model.

The mid-P variant of Fisher's exact test is a continuous descriptive metric that is based on Fisher's exact test and uses analytical probabilities of co-occurrence to describe associations, based on species occupancy and the number of samples. It is the analytical equivalent of a fixed-equiprobable null model, which was used here for efficiency and to avoid under-randomization. Unfortunately, as of yet there is no equivalent analytical solution to a fixed-fixed randomization null model. Fisher's exact test was recently repurposed as an analytical approach for categorizing species associations as positive, negative, or random (*45*). We used the mid-P variant of Fisher's exact test because we were interested in a continuous metric that can be compared across associations rather than categorizing and counting association types using a significance threshold. The mid-P variant of Fisher's exact test describes the probability of two species co-occurring at any number of sites, given their frequencies of occurrence and the number of sites (based on simple combinatorics). The metric comparatively scores the strength of each association on a continuous scale by splitting the probability distribution at the observed number of mutual occurrences for each pair. This produces values near 0.5 for pairs that co-occur the expected number of times, values > 0.5 for species that are positively associated (or aggregated), and values < 0.5 for pairs that are negatively associated (or segregated). The output scores vary between 0 and 1, non-inclusive. Raw scores are then transformed to z-scores using the base R function qnorm, which are useful because they vary from positive to negative infinity, placing random scores near 0. One advantage of z-scores is that they emphasize variations in strong interactions (e.g. the difference between 0.990 and 0.999 is given more weight than the difference between 0.790 and 0.799 because this difference is harder to achieve mathematically). They also provide a way to subtract association scores (which we do in our separation of biotic and abiotic variables, see next section), because they are unbounded, while the raw scores are restricted to values between 0 and 1. Recently, Harris (*46*) introduced new methods for inferring indirect effects and networks of species interactions from co-occurrence data. However, Harris' method assumes that all species in the analysis are potentially interacting indirectly through a connected network (e.g. three-way interactions involving the regulation of associations by third parties). The null model analysis used here is a simpler measure of the degree of direct pairwise positive and negative associations. We will refer to the z-transformed output of the mid-P variant of Fisher's exact test as association weights, and as aggregation and segregation weights when referring to the weights of positive and negative associations.

Mutual potential range co-occurrence analysis

To determine the strength of abiotic effects on associations over time, we ran a co-occurrence analysis on potential range sites shared between each species in a given pair (termed mutual potential range, M_{ij}). We used the potential ranges previously estimated for each species (P_i). For each pair, we extracted the subset of sites falling within the potential ranges of both species in the pair ($M_{ij} = P_i \cap P_j$) (*26*).

Because sample size can affect the outcome of association weight calculations, we included only pairs that had at least 10 sites in their mutual potential ranges (enough to perform a co-occurrence calculation, but not so many as to exclude a majority of pairs). The original association weights were recalculated using 10 randomly chosen sites from the current subsample of 60 sites, as described above in the co-occurrence analysis section, and the mutual potential range associations were calculated using 10 sites randomly chosen from within the mutual sites present in the subsample. The original associations were then separated into two components, such that the association weights of the components sum to the original association weight: (1) the biotic component, calculated using sites in each pair's mutual potential range (because associations within mutual potential ranges cannot be driven by dispersal ability or the climate variables used to calculate their limits, see Fig. S3); and (2) the abiotic component, computed by calculating the difference between the original association and its biotic component. We treat the biotic and abiotic components as species pair associations in their own right, and the sum of their weights is equivalent to the association weight of the full associations.

The biotic component includes potential mechanisms such as direct and indirect biotic interactions and range dynamics. The biotic component can also be impacted by selection between time bins (*21*). The abiotic component is strictly a result of the factors used to calculate the mutual niche space (geographic coordinates, mean annual precipitation, mean annual temperature, and seasonality variables). In theory, this means that the biotic component could also be affected by a climate variable that we have not factored out in this analysis. However, for such a variable to have an appreciable effect on our results within the mutual potential ranges of species pairs, it would have to impact species occurrence consistently across the continent, in a fashion comparable to mean annual precipitation or mean annual temperature without covarying with them. The association weight and abundance of aggregations and segregations for each component was compared with those of the full associations.

If the included abiotic variables (mean annual temperature, mean annual precipitation, seasonality of temperature and precipitation, and geographic coordinates) strongly regulate the association of a given pair, the association within the mutual potential range will be weaker than the original association strength because the sites included in the recomputed mid-P variant of Fisher's exact test will no longer harbor that abiotic signal. For example, if two species are segregated due to disparate climate preferences, the original association will be negative, but species should associate randomly inside of the mutual potential range, indicating that climate fully accounts for the association. If a pair aggregates in sites with high mean annual temperature, using the mutual potential range (i.e., removing the sites with low mean annual temperature where neither species occurs) will reduce the strength of the original aggregation by removing mutual absences. The reasoning for the mutual niche analysis is summarized visually in Fig. S3.

The comparison between the original and mutual potential range association scores identifies three broad categories of pairs, corresponding to the three panels in Fig S3. (A) Abiotic

variables fully explain the spatial relationship of the pair. (B) Abiotic and biotic variables both influence the spatial relationship of the pair. (C) Abiotic variables do not explain the spatial relationship of the pair. In the first case, the association within the mutual potential range is random and its z-score is close to zero. In this scenario, the original score minus the biotic score will be close to the original score, indicating that abiotic factors are driving the relationship (Fig. S3A). If biotic and abiotic variables are both contributing to the relationship, then the biotic component will be estimated by the weight calculated from the mutual potential range, and the difference between the original and biotic weights will indicate the extent of abiotic component (Fig. S3B). If biotic and abiotic components work in the same direction (e.g. both cause segregation), then their absolute values will add up to the absolute value of the original score. However, it is possible for the biotic and abiotic components to drive spatial patterns in opposing directions. If this is the case, a positive and negative value may yield an overall association that appears weak (association z-score close to zero; Fig. S3B). In the final case, the biotic component will be almost the same as the original association, indicating either that the pattern is only evident inside the mutual niche, or that the mutual niche is almost as large as the full potential range of both species (Fig. S3C). Either way, the abiotic component will be left with a number close to zero when the biotic score is subtracted from the original.

The analysis revealed that the use of mutual potential range sites causes many original association strengths to decrease or flip, indicating abiotic regulation of community assembly. This is the most common case in all three time intervals. However, the end-Pleistocene aggregations were stronger and more frequent when abiotic variables were factored out, suggesting enhanced biotic regulation of co-occurrence when the megafauna were still alive (Fig. 3A-B, G-H).

Relative magnitude of biotic vs. abiotic components

We compared the average magnitude of biotic and abiotic components to establish their relative importance in community assembly. Both biotic and abiotic components were important in all time intervals, but the magnitude of the biotic component decreased from the end-Pleistocene to the Holocene and stayed consistent into the Recent (Fig. 4). The magnitudes of biotic and abiotic components reinforce the conclusion that abiotic control of community assembly processes is important but did not vary strongly over time. By contrast, the importance of the biotic component decreases after the end-Pleistocene. This result suggests that biotic factors structured end-Pleistocene communities to a greater degree than subsequent time intervals, and this partly drove the loss of aggregations in the following intervals.

Supplementary Text

Statistical confounding factors

Measurements of co-occurrence can be influenced by certain characteristics of the input matrix. The most common confounding factors are the number of sites and the variance in sampling intensity. Sampling intensity can in turn influence apparent occupancy of species and the richness of sites in a dataset. Of course, biological changes in occupancy and richness also control co-occurrences patterns and should be interpreted as a real signal. Co-occurrence analyses attempting to compare associations calculated from data with varying number of sites and sampling intensity should take measures to account for each of these factors.

Number of samples. Time periods with more sites yield stronger statistical power and may artificially create stronger associations relative to assemblages with fewer sites. We employed a subsampling procedure to ensure that the same number of sites was used for the calculation of pairwise associations we wished to compare (e.g., association strength distributions across time intervals). To compare full associations across time intervals, we subsampled each time interval to the same number of sites and repeated the process 1000 times. The number of sites in each subsample is somewhat arbitrary, but should be no greater than the number of sites in the least-sampled interval (Pleistocene), as subsampling was run without replacement. Sub-sampling below the sample size of our least-sampled interval allows us to estimate variance of our results within all sampled intervals. We ran our analyses fixing the subsample size at 48, 60, and 72 (the latter is the total number of sites available in the end-Pleistocene). The subsample number did not substantively change our results. Although there were differences in the weights of individual pairs, this translated to only very small changes in the proportions and average weights of aggregations and segregations in each subsample. The overall temporal patterns (i.e. increase in segregation weight and proportion in biotic associations and the opposite in abiotic associations) remained constant. The analyses presented in the main text are based on subsamples of 60 sites. The figures for the co-occurrence analysis with 48 and 72 sites in each subsample were so similar to our main text results (i.e. Figs 3 and 4) that we felt it would be redundant to include them here.

Sampling variance. Variance in the sampling intensity between time intervals can also create artificial differences. In particular, sampling intensity affects the marginal totals of a data matrix (occupancy = row sums and site richness = column sums). The closer the occupancies of species in a pair are to 50%, the stronger the power of co-occurrence tests. Increased sampling intensity resulting in higher site richness may, but does not necessarily, lead to overestimation of positive associations in comparison to a dataset with lower sampling intensity. It is difficult to determine the extent to which site richness and species occupancy patterns reflect biological changes vs. sampling effects. However, we can estimate the effects that occupancy and richness have on the outcome of associations by running randomization analyses (i.e., null models) with these features fixed (i.e. fixed row sums or column sums). If the outcome of the randomizations differs from the outcome of the empirical dataset, we can assume that the distribution of species pair associations is not an artefact of the marginal totals of the matrix, regardless of whether or not the marginal totals are influenced by sampling intensity.

We implemented a fixed-equiprobable randomization (*47*) of the subsampled matrices (R package EcoSimR (*48*)), which preserves species occupancy while randomizing the actual sites of occurrence. We also implemented an equiprobable-fixed randomization, which preserves site richness instead. We avoided fixed-row and fixed-column sum randomizations to avoid the problem of under-randomization (*49*, *50*). Association weights for each pair were extracted from the randomized matrices. We examined the density distributions of randomized associations over time to establish expectations. See Fig. S8 for an explanation of how to interpret density distributions. The difference in occupancy over the time intervals (or any sampling bias causing apparent occupancy shifts) predicted the strengthening of association scores (a decrease in the height of the center peak and increases in the left and right peaks). However, these factors do not explain the shift toward negative associations that is the central result of this paper (Fig. S9). They also predict an increase in the proportion of aggregations, which is opposite to the results in this paper. Site richness predicted slightly stronger positive associations in the end-Pleistocene,

but was unable to predict the excess of strong positive associations in this interval and the excess of strong negative associations in subsequent intervals (Fig. S9).

Ideally, we would like to know whether and to what extent occupancy and site richness have changed biologically (versus from sampling inconsistencies) over our time intervals. We approached this question qualitatively and quantitatively. Qualitatively, we can check for alignment with a priori knowledge about each time interval. For example, previous research shows that there was competitive release in the Holocene as a result of the extinctions (*29*). This suggests that survivors should increase in abundance and occupancy in the Holocene. We observe an increase in the occupancy of common species, which aligns with this prediction. We also know that the end-Pleistocene had much higher gamma diversity than the later time intervals due to the presence of megafaunal species across the continent. As such, we should be unsurprised to find end-Pleistocene sites have a higher maximum richness.

A quantitative way to evaluate the effects of sampling is to estimate the number of species occurrences missing in our datasets and evaluate in missing data through time. To do this, we first used correspondence analysis and coherence (*51*, *52*) of the assemblages to estimate the number of false negatives: the number of species occurrences missing from our datasets that should likely be presences. Previous research has supported the notion that species are often arrayed according to several overlapping gradients (*53*), and as such, species absences at sites surrounded by presences (when the sites are ordered according to an environmental gradient) are unlikely to represent true absences. We counted embedded absences (absences surrounded by presences) with the sites arranged according to each of the first three axes of the correspondence analysis (because the eigenvalues of the correspondence analysis indicated three dimensions of organization). This was done separately for each of the three orderings. We then evaluated how many of the embedded absences were found all three times (triply absent), which mostly likely represent false absences (false negatives). The count of triply embedded absences divided by the sum of presences plus embedded absences is then the percent of the estimated total occurrences that is missing (false negatives). False negatives were most common in the recent (46.97%), lower in the Holocene (43.41%), and lowest in the end-Pleistocene (30.17%). Occupancy changes are in the opposite direction than we would expect from these results, including increases in the occupancies of several common species in the Holocene and Recent. Thus, we conclude that the occupancy changes are driven by biological mechanisms (not statistical artefacts), and therefore that our results are not being driven by sampling. In sum, changes in marginal totals cannot fully explain our results, and changes over time of marginal totals in our data are unlikely to be caused by sampling biases. Therefore, any influences of marginal totals on our results are probably biological rather than artefacts of sampling. Matrix fill, which can influence the strength of associations, was lowest in the end-Pleistocene and highest in the Recent. Nonetheless, the rate of false negatives was lowest in the end-Pleistocene interval. This suggests that our conclusion that marginal totals have changed biologically rather than by sampling biases applies to matrix fill as well. Furthermore, lower matrix fill should cause weaker associations, so change in matrix fill cannot explain the directional shift that is the focus of this paper.

Occupancy

The distribution of mammalian occupancy changed from the end-Pleistocene to the Holocene (Fig. S10). The end-Pleistocene was characterized by many species having low- (<5%) to mid-occupancy (5 – 20%) The high number of species with the lowest occupancies partially

persisted into the Holocene, but the number of species at medium occupancies decreased dramatically, with most surviving species moving toward occupancies above 20% or below 5%. The Holocene occupancy distribution also expanded to include higher-occupancy species (end-Pleistocene, Holocene, and Recent maximum occupancies are 43, 55, and 59%, respectively), while occupancies of rarer species decreased (Fig. S10). As a result, the median occupancy dropped from 7.0% in the end-Pleistocene to 4.1% in the Holocene, but the mean occupancy increased from 9.3% to 12.8%. Species occupancies for survivors across consecutive intervals was highly significant ($p < 0.001$) for both transitions (end-Pleistocene to Holocene, Holocene to Recent), but end-Pleistocene occupancy only partly explained variation in Holocene occupancy ($r^2 = 0.60$; Fig. 1A), while Recent occupancies closely tracked Holocene occupancies ($r^2 = 0.93$; Fig. 1B).

Taphonomy

The depositional environments of the sites in each time interval could influence the results of this study, especially if particular environments are differentially represented within the three time periods. The sites analyzed here come from a variety of depositional systems, including cave sites and several types of surface assemblages. Cave or karst bone assemblages are formed in many different ways and may be dominated by smaller-bodied mammals as a result of accumulation by owls (*54*), or because of the relatively small size of species that usually inhabit caves (e.g., bats). Many cave sites also include larger animals, however. The subset of FAUNMAP sites used in this paper includes several dozen cave assemblages with 10 or more species of mammals larger than 1 kg, and these are distributed across all three time intervals.

If cave assemblages in our study are biased toward smaller mammals, a time interval with a higher proportion of cave sites might be expected to exhibit weaker aggregations. This is because many smaller mammal species typically have lower occupancies (i.e. smaller ranges) than larger mammals (*55*, *56*). Therefore, they might not associate strongly with other species. If the Holocene and Recent have more cave sites than the Pleistocene, then taphonomy could drive the observed pattern toward weaker apparent positive association. We find that 40% of the end-Pleistocene sites and 51% of the Holocene sites are caves, while only 19% of Recent sites are caves. Although the Holocene does have slightly more cave sites than the end-Pleistocene, the Recent has many fewer. Nonetheless, the Holocene and Recent produce similar co-occurrence results that differ from end-Pleistocene co-occurrences. This indicates that taphonomic processes resulting in body size biases in cave fossil assemblages have not affected our results.

Biogeography

Maps of our Pleistocene, Holocene, and Recent sites are presented in Fig. S1. The sites in all time intervals are restricted to the US and southern Canada. The density of sites is higher in the younger time intervals, but this is accounted for by our subsampling protocol, which summarized results from 1000 runs in which each time interval is subsampled to the same number of sites. Visual inspection of the maps reveals that there is a lack of Pleistocene sites in the northern mid-west and northwest of the US, resulting in a reduction of the total geographic area covered by our sites in the end-Pleistocene interval (6.6 million km^2, estimated with a minimum convex polygon, disregarding coastlines) compared to the Holocene (13.9 million km^2) and Recent (11.7 million km^2) intervals. These areas were covered by glaciers in the Pleistocene, so if the change in extent caused changes in co-occurrence, it should be interpreted as a real biological signal and is factored into our analysis of abiotic variables. We use

hypervolumes and convex hulls on species occurrences to estimate species niches in this study, and the presence of glaciers covering entire regions could cause large over-estimates of species geographic ranges in the end-Pleistocene. However, because end-Pleistocene ranges are consistently smaller than Holocene and Recent ranges, correction for this factor would only strengthen our results. Survivors and victims in the end-Pleistocene are subject to the same biases, and so their comparison should not be systematically biased by the presence of glaciers. Finally, the mutual potential range analysis does not suffer from bias imposed by glacier coverage, as there are no sites in these areas, and thus they cannot be counted in the mutual niche of any pair.

The distribution of geographic ranges across the time intervals correlates with the total amount of area available in each time interval (compare areas cited above with Figs. S5B and S7B), and a similar relationship is evident with the four-dimensional climate envelope hypervolumes (31.1, 84.5, and 27.6 z^4 for the end-Pleistocene, Holocene, and Recent, respectively; compare with Figs. S5A and S7A). It is possible that changes in niche breadth were simply a result of retreating glaciers and climate change, but such a simple explanation would only be supported in the unlikely event that all niche expansions take advantage of new niche space only. When geographic and climatic envelopes were plotted as a ratio of available background variation (Figs. 2 and S5), the pattern of expanding Holocene niches was still evident. This indicates that Holocene mammals filled a larger percent of the available climate space than the same species in the end-Pleistocene. Such expansions suggest that the competitive release scenario we discussed in our main text allowed some species to fill newly available niche space as well as existing niche space in the absence of competition or predation from extinct end-Pleistocene megafauna and is consistent with the central message of this paper.

Time-averaging

There are three related types of time averaging that could affect the outcome of this analysis: (a) Because increases in time-averaging may correspond to increases in richness, the number of species recovered may be increased in sites with a longer duration between minimum and maximum ages. (b) Binning sites from different times into broader time intervals place sites that may not be strictly contemporaneous in the same matrix, and (c) the three time intervals explored here (end-late Pleistocene, Holocene, Recent) are not the same duration. These three types of time averaging are each addressed below.

If sites have minimum and maximum dates that are farther apart, time-averaging may cause some species to appear at the same sites that did not truly co-occur. This would cause species pairs to appear more aggregated in intervals where sites have broader age ranges. End-Pleistocene sites had an average duration of 5418 years, Holocene sites had an average duration of 2877 years, and Recent sites had an average duration of 385 years. We do see more frequent and stronger aggregations in the end-Pleistocene, which has the least precisely dated sites. To address this potential bias, we ran a version of the co-occurrence analyses from which we removed end-Pleistocene sites with higher richness than the richest site in the Recent interval with a duration less than 400 years. This ensures that all site faunas could have accumulated in 400 year period (maximum 21 species). The analysis yielded similar results (Fig. S11) to those presented in the main text.

If sites that are not strictly concurrent are analyzed as parts of a single interval, the pattern of presences and absences that drive the association results must be consistent temporally (within the interval) as well as spatially to receive strong weights (i.e. high positive or negative Fisher's

Exact Test mid-P z-scores). In other words, the binned time interval represents a spatiotemporal relationship for each pair rather than a strictly spatial one, and the association must be occurring in space as well as time to exhibit a strong pattern. In a practical sense, this is true for any fossil dataset, because most fossil assemblages take time to accumulate. In practice, the association weights calculated for a time interval of any given duration represent the spatial relationship of pairs over that duration, averaging out any variations in the relationship that may have occurred over time. Thus, if associations do change over the duration of the binned interval, time averaging could cause such pairs to appear random. The more dynamic the association pattern, the weaker we expect associations to be. The longer the time interval, the more likely that it encompasses temporal changes in associations and thus the weaker we expect the pairs to be. If this scenario was driving our results, we would expect the end-Pleistocene and the Holocene to exhibit weaker associations than the Recent, but we observe that the Holocene and Recent have similar associations.

Finally, the Holocene and end-Pleistocene intervals have roughly the same duration (9.7 and 9.3 ka, respectively) while the Recent interval is much shorter (2 ka). Despite this, the greatest differences in co-occurrence are observed over the Pleistocene to Holocene transition. This indicates that time averaging is not responsible for the patterns detected in our analyses. Nonetheless, to firmly rule out the idea that time averaging is responsible for the aggregations observed in the end-Pleistocene, we ran our co-occurrence analyses again with sites older than 18 ka excluded, effectively reducing the duration of the end-Pleistocene interval to 7 ka. The temporal co-occurrence patterns in Figs. 3 and 4 were unchanged. This analysis demonstrates that longer time-averaged intervals do not necessarily translate to stronger aggregations.

Radiocarbon dating

Radiocarbon dates can be compromised by contamination of modern carbon (*57*, *58*). The influence of contamination becomes larger with the increasing age of the dated sample (i.e., a 1-2 ka discrepancy for 0-10 ka sites and 2-4 ka discrepancy for 10-25 ka sites with 2% contamination). The potential inaccuracies in our radiocarbon dates may cause our sites to be aligned with the incorrect climate layers in our hypervolume analyses, and this mismatch may be more frequent in the Pleistocene dataset than the Holocene and Recent datasets. Therefore, differences in the abiotic signal in the end-Pleistocene might be caused by incorrect ^{14}C dates. However, the direction of the dating inaccuracy caused by contamination is consistently toward a younger age, typically meaning that the true site age is 0-4 ka older than its calculated age. To address this issue, we ran our biotic/abiotic analyses with coarsened climate data, where each site was assigned climate means averaged across its apparent CCSM3 1000-year interval and the three intervals preceding it. Because Pleistocene sites are most likely to be dated incorrectly, this approach gives Pleistocene sites a much greater chance of having accurate—if less precise—climate estimates. Simultaneously, it weakens the accuracy and precision of Holocene and Recent climate estimates (i.e., because Holocene sites are not likely to have more than 1 ka discrepancy, and therefore were probably assigned the correct climates to begin with), thus placing the time intervals on more equal footing.

It is also possible that accurate dating of sites might be degraded by the procedures used by FAUNMAP, e.g., assigning the same dates to loosely associated macrofossils or using bulk dating methods. Therefore, it is possible that the dataset contains random instead of systematic bias in dating errors. To address this issue, we randomly selected either the minimum or maximum age of each site to align with climate layers and re-ran the hypervolume analyses,

repeating the process five times. This approach is highly conservative because it shows whether or not the dating uncertainties have the capacity to overturn our results. By randomly choosing the minimum or maximum age of each site, we may also shuffle sites along the environmental gradient, and this can influence the outcome of the estimated niche spaces. Neither analysis changed our results. This sensitivity analysis suggests that spatial gradients in climate are relatively stable even when large shifts are occurring over time (e.g. site A is always warmer/colder than site B), lending robustness to these results.

Results of radiocarbon dating sensitivity analysis

The results of the dating sensitivity analysis were not substantively different from the results presented in the main text. The original analysis used 1000-year climate layers to assign climate variables to each site. The median (rather than mean) magnitude of aggregations and segregations is presented in Fig. S12, to ensure that our results are not influenced by the distributions of association scores, which may be strongly skewed when aggregations and segregations are plotted separately. We present our results for climates assigned according to 4000-year averages in Fig. S13. Note that the average weight of aggregations decreases in the original associations and in the biotic component, while the abundance and weight of segregations increases. The opposite pattern is evident in the abiotic component, and this is consistent with the results presented in the main text. The results do not change when sites are assigned climates from their minimum or maximum date at random (Fig. S14). In Figs. S15 and S16, the average relative association weights for biotic and abiotic factors are presented when calculated with 4000-year averages and minimum/maximum dates, respectively. The decrease in biotic regulation over the Pleistocene-Holocene transition is upheld. However, it appears that abiotic regulation may also have decreased slightly. Although the patterns in the full associations seem to have been weakened slightly, it is still clear how they were formed: (1) a decrease in the importance of biotic regulation with respect to abiotic regulation, and (2) a shift of biotic regulation toward segregations.

Excluded survivor-survivor pairs

The results presented in the main text are based on pairs with at least 10 mutual niche sites. However, the pairs excluded by this threshold are theoretically separated by abiotic factors, namely, differential habitat preferences or inability to disperse into one another's niches. Thus, it may be informative to examine how many pairs do not have sufficient overlapping potential ranges in each time interval. The percent of pairs excluded was 67.2, 68.5, and 58.4 for the end-Pleistocene, Holocene, and Recent, respectively. This percent is calculated on subsamples of pairs, so this means that the average pair was excluded roughly 60% of the time it was present in the 1000 iterations. These numbers suggest potential range overlap increased in the recent. This agrees with the increasing climate-driven aggregation and decreasing segregation we observe in the results for pairs that do have 10 or more sites in their mutual potential ranges (Fig. 3A-B), thus strengthening our results.

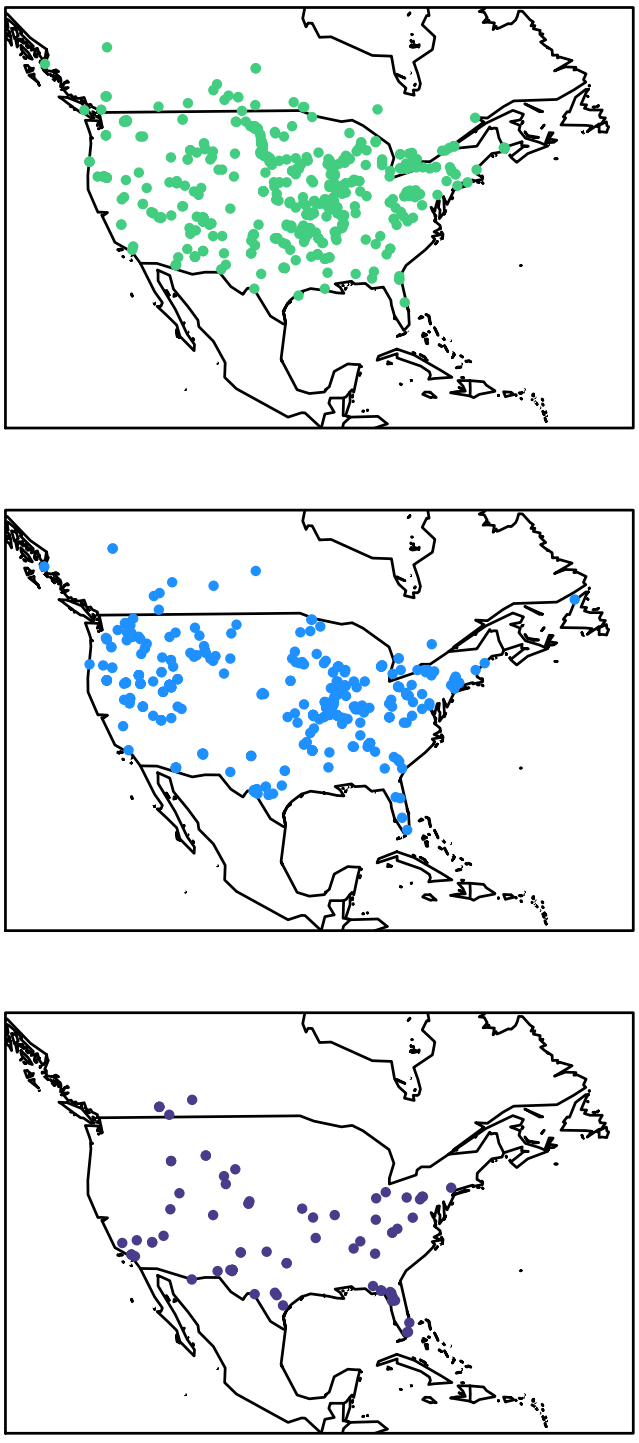

Figure. S1.

Maps of sites used in our analyses. Recent (top: 535 sites), Holocene (middle: 381 sites), and end-Pleistocene (bottom: 78 sites) intervals.

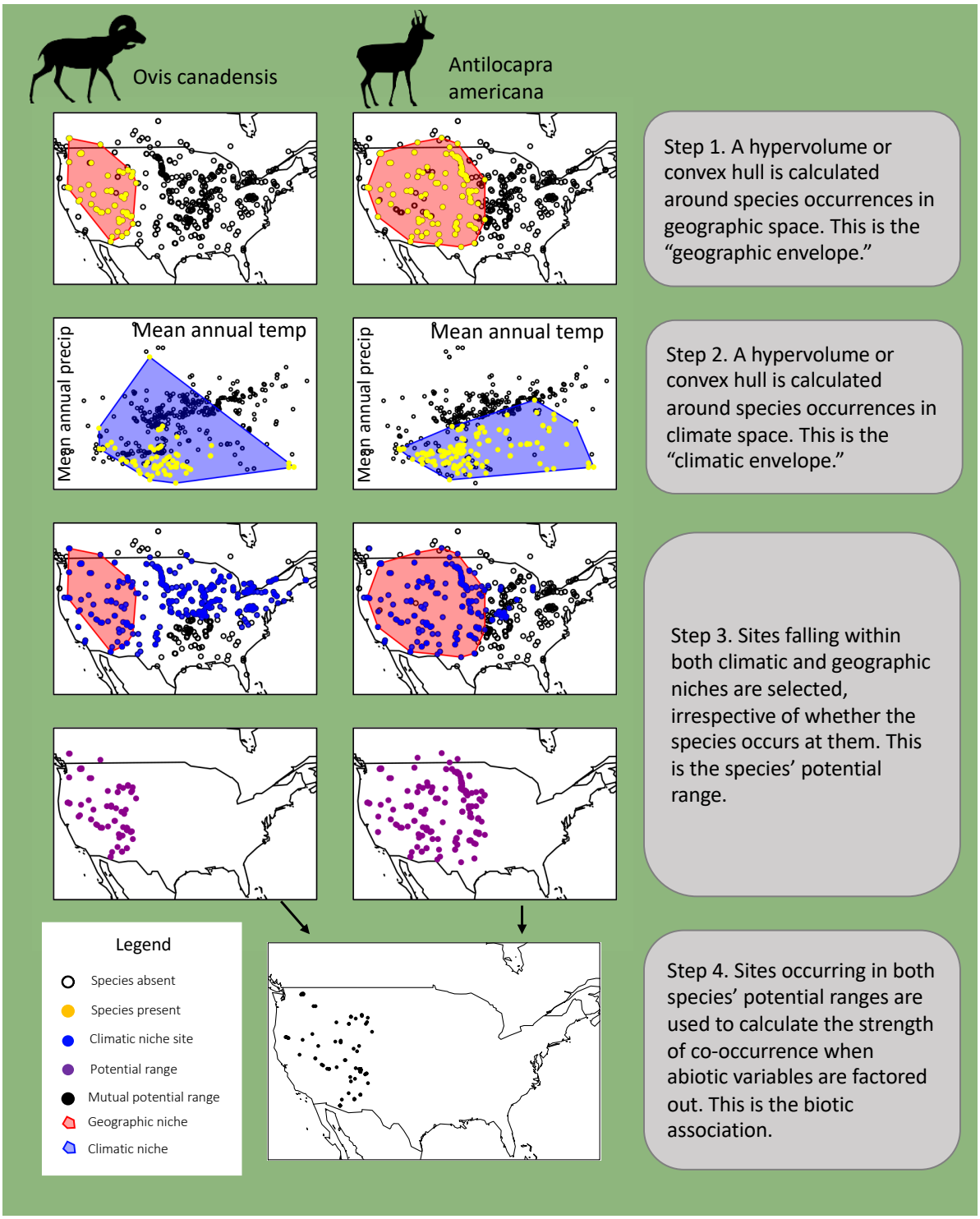

Figure. S2

Calculation of mutual potential range sites for an example pair. This schematic illustrates the process of selecting the mutual potential range sites of an example pair. Mutual potential range sites are used to calculate the biotic component of associations.

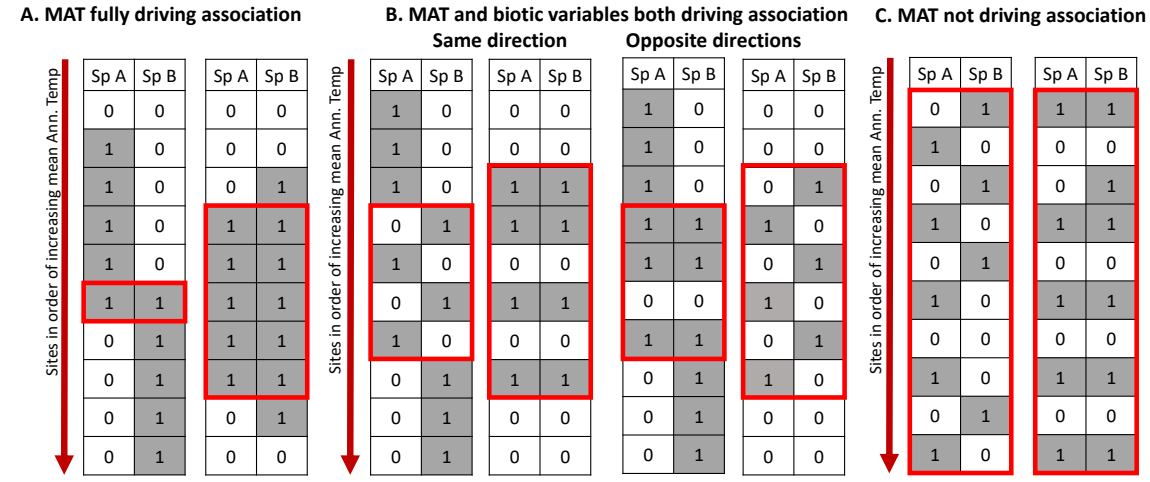

Figure. S3

Explanation of the mutual potential range calculation. Example calculations of biotic and abiotic components across a hypothetical set of sites, simplified to one abiotic variable for clarity (sites are ordered vertically in order of increasing mean annual temperature). Three scenarios are depicted for segregation (first table of each pair) and aggregation (second table in each pair). The second scenario has two additional tables depicting hybrid situations. (A) Mean annual temperature is responsible for the association. (B) Mean annual temperature is partially responsible for the association. (C) Mean annual temperature does not explain the association. The association weight is calculated first for the full set of sites and then for the mutual potential range (red rectangle). In scenario (A), the biotic score is strongly reduced in absolute value (compare full to biotic association weight). In (B) the score is somewhat reduced or flipped when biotic and abiotic regulators are acting in the same direction. When regulators are acting in opposite directions, there is no predictable pattern but component scores have opposite signs and may be stronger (absolute value) than the full association weight. In (C) the score is not reduced, and it may increase. Associations observed only within the mutual potential ranges cannot be attributed to the abiotic variables being tested.

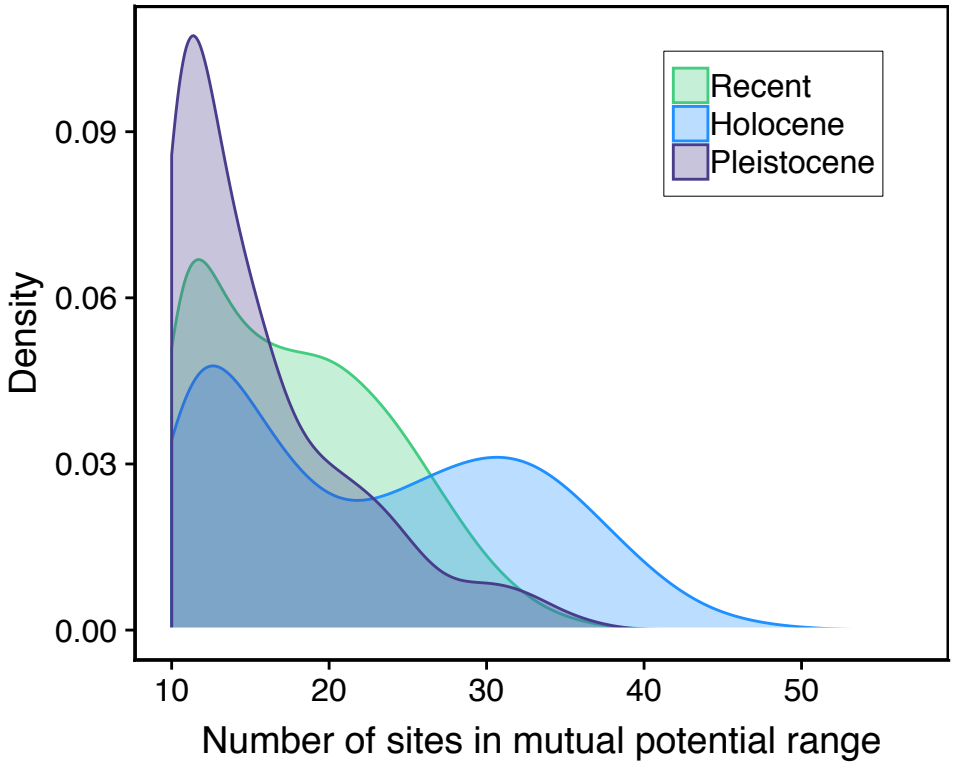

Figure S4.

Number of sites in the mutual potential ranges. Number of sites in M_{ij} of each pair over the three time intervals for pairs with at least 10 mutual potential range sites. Mutual potential ranges are calculated on subsamples of 60 sites to standardize sampling, so 60 is the maximum overlap. All else being equal, an increase in the number of mutual potential range sites causes an increase in the strength of abiotic aggregations and a decrease in the strength of abiotic segregations, because it results in more mutual absences in the full set of sites and fewer sites where one species in the pair occurs without the other.

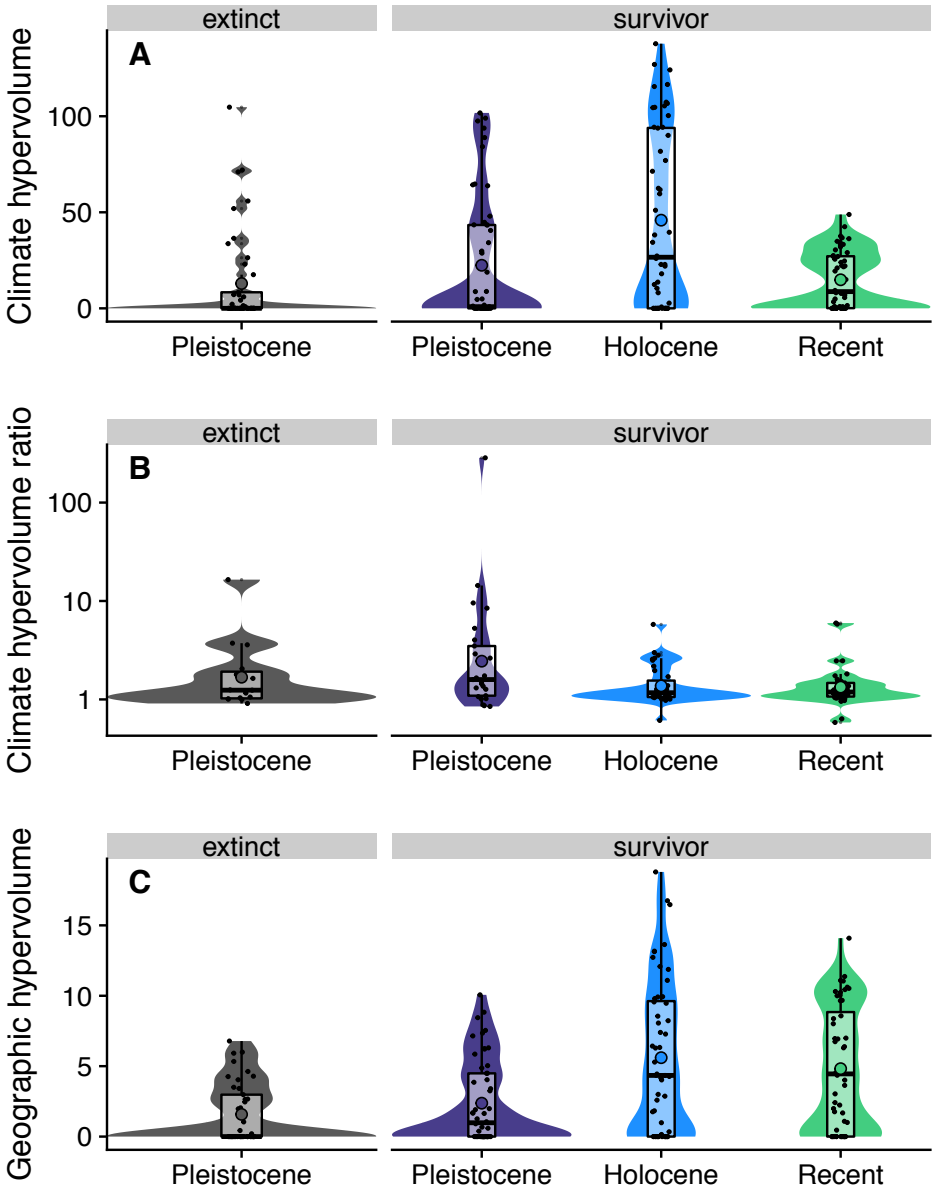

Figure. S5

Niche hypervolumes. (A) Climatic envelope of each species calculated from occupied sites inside its geographic hypervolume in each time interval. (B) Climatic envelopes in A as a ratio of the climate envelope calculated from unoccupied sites inside each species' geographic hypervolume in each time interval. (C) Geographic envelope of each species by time interval. Species climatic hypervolumes include mean annual temperature, mean annual precipitation, temperature seasonality, and precipitation seasonality. Geographic hypervolumes are constructed from projected equal-area geographic coordinates. Shaded areas represent density distributions with a total area of 1.

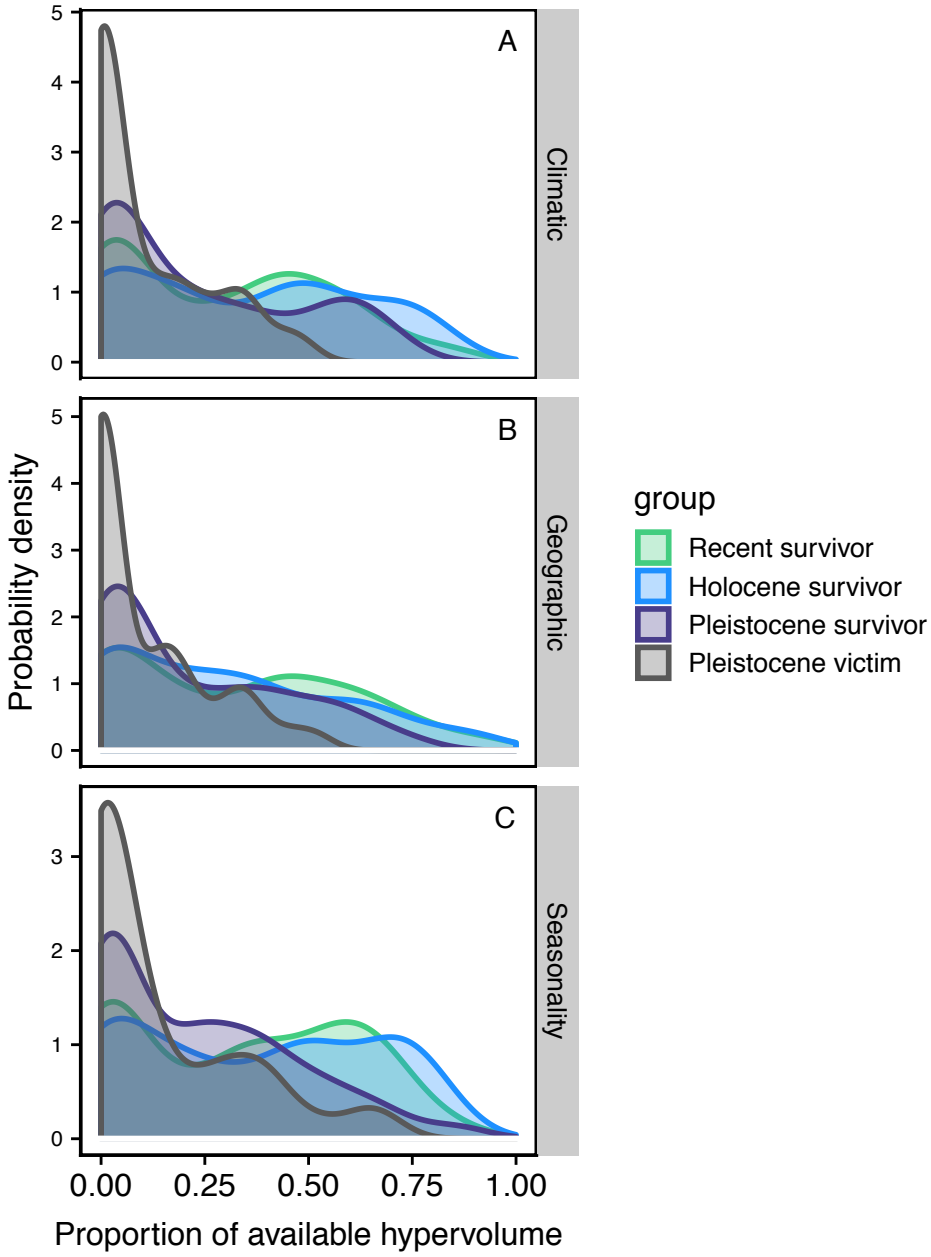

Figure S6.

Relative niche areas. Density distribution of geographic, climatic, and seasonality convex hull areas, as a proportion of total background variability in each time interval.

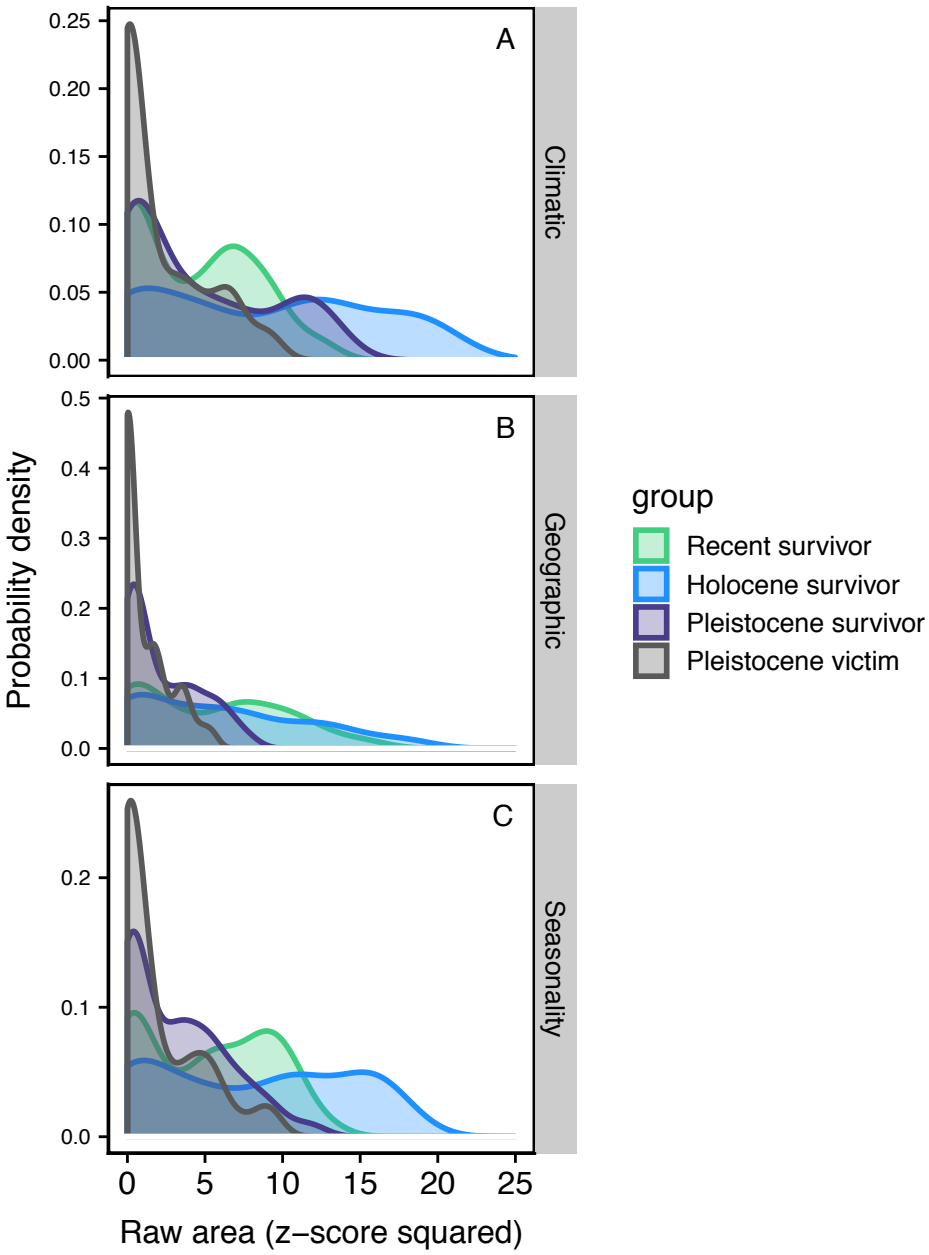

Figure S7.

Raw niche areas. Density distribution of climatic, geographic, and seasonality envelope areas in the time intervals, calculated with convex hulls. The raw areas are displayed, without accounting for background variation.

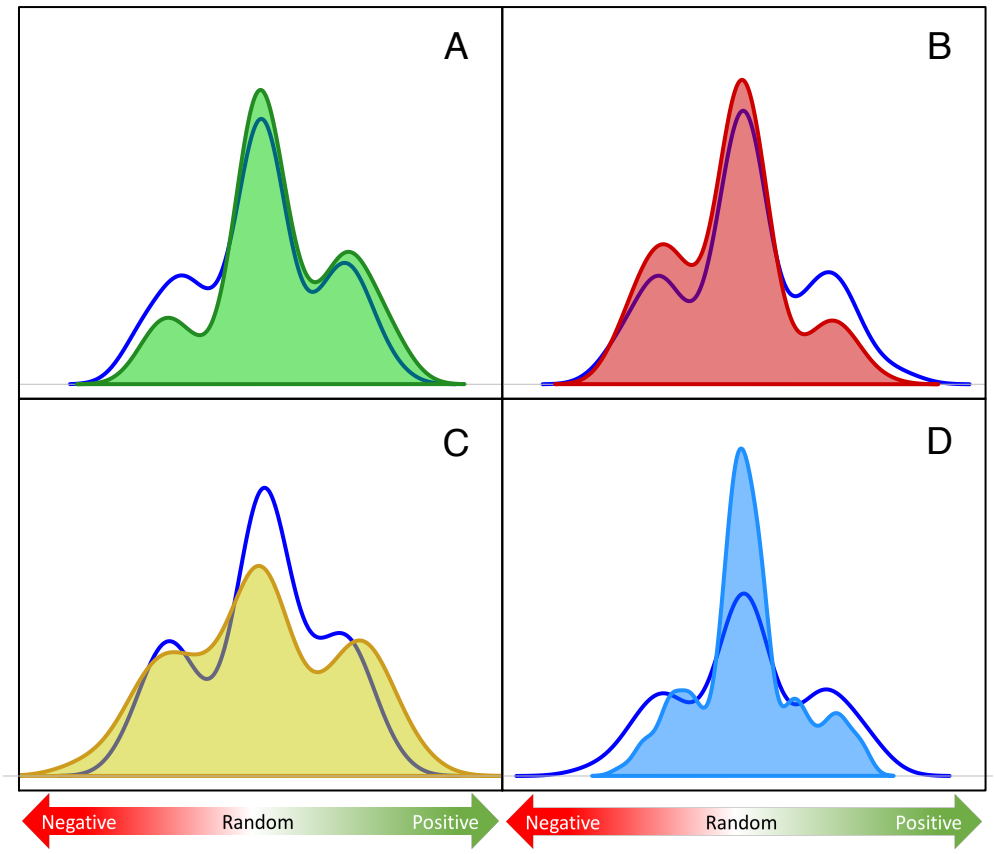

Figure S8.

Illustrated scenarios for systematic shifts in co-occurrence. Expectations for the density distribution of association scores are plotted in the presence of systematic community shifts in a hypothetical structured assemblage. Dark blue line indicates a baseline expectation for the distribution of co-occurrence scores, with weak associations falling in the center peak, and strong positive and negative associations represented by the right and left hand peaks, respectively. Panels show the expected change in the case of a hypothetical shift toward (A) positive associations; (B) negative associations; (C) stronger associations; and (D) weaker associations. Note that the center peak does not move on the x-axis; changes are indicated by a combination of shifts in the left and right peaks or changes in the height of any peak.

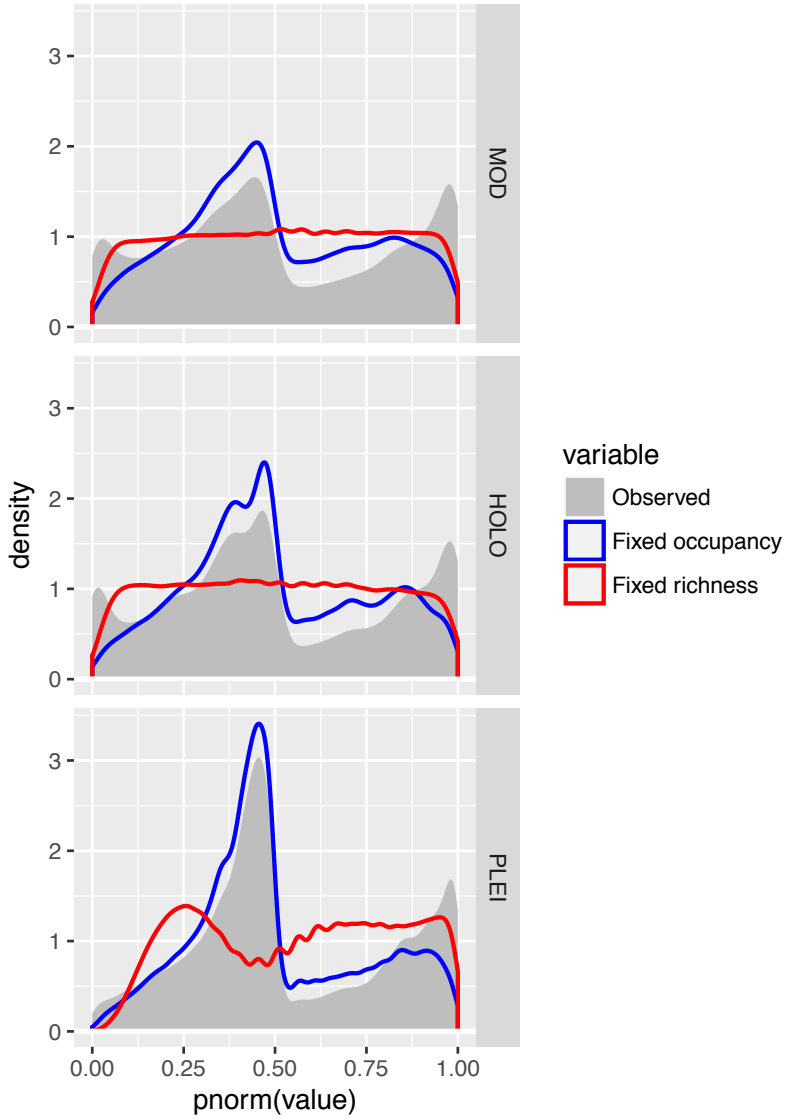

Figure S9.

Randomization test results for sampling bias. Kernel density plots of the distribution of large mammal association weights (derived from the mid-P variant of Fisher's Exact Test) within the end-Pleistocene (bottom), Holocene (middle), and Recent (top) when matrices are randomized using fixed species occupancy with equiprobable site richness (blue) and equiprobable species occupancy with fixed site richness (red) randomization. This indicates the expected result if association scores purely result from changes in occupancy or site richness, since row and column sums are fixed, respectively. Shaded gray areas represent the observed distribution of association weights in each time interval.

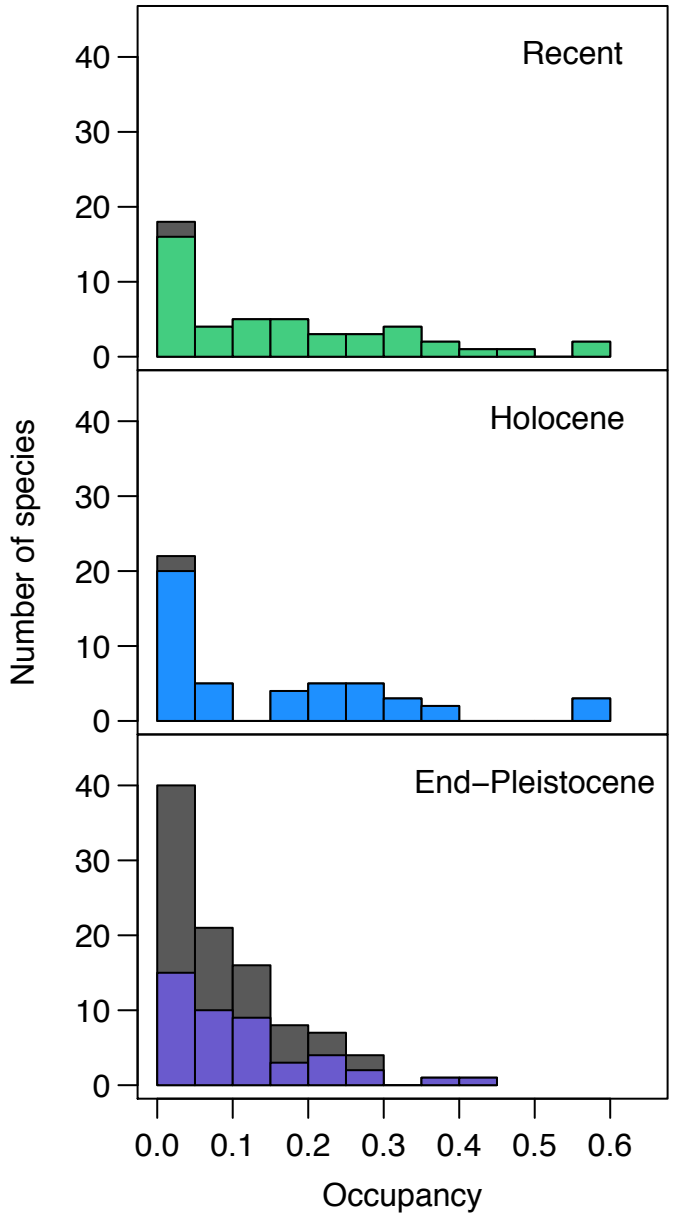

Figure S10.

Occupancy distributions of mammals in the three time intervals. Gray bars represent species that are recorded only within one time interval. For the Holocene and Recent intervals these are rare or low-density species that are not commonly sampled, while for the end-Pleistocene all are extinct megafauna.

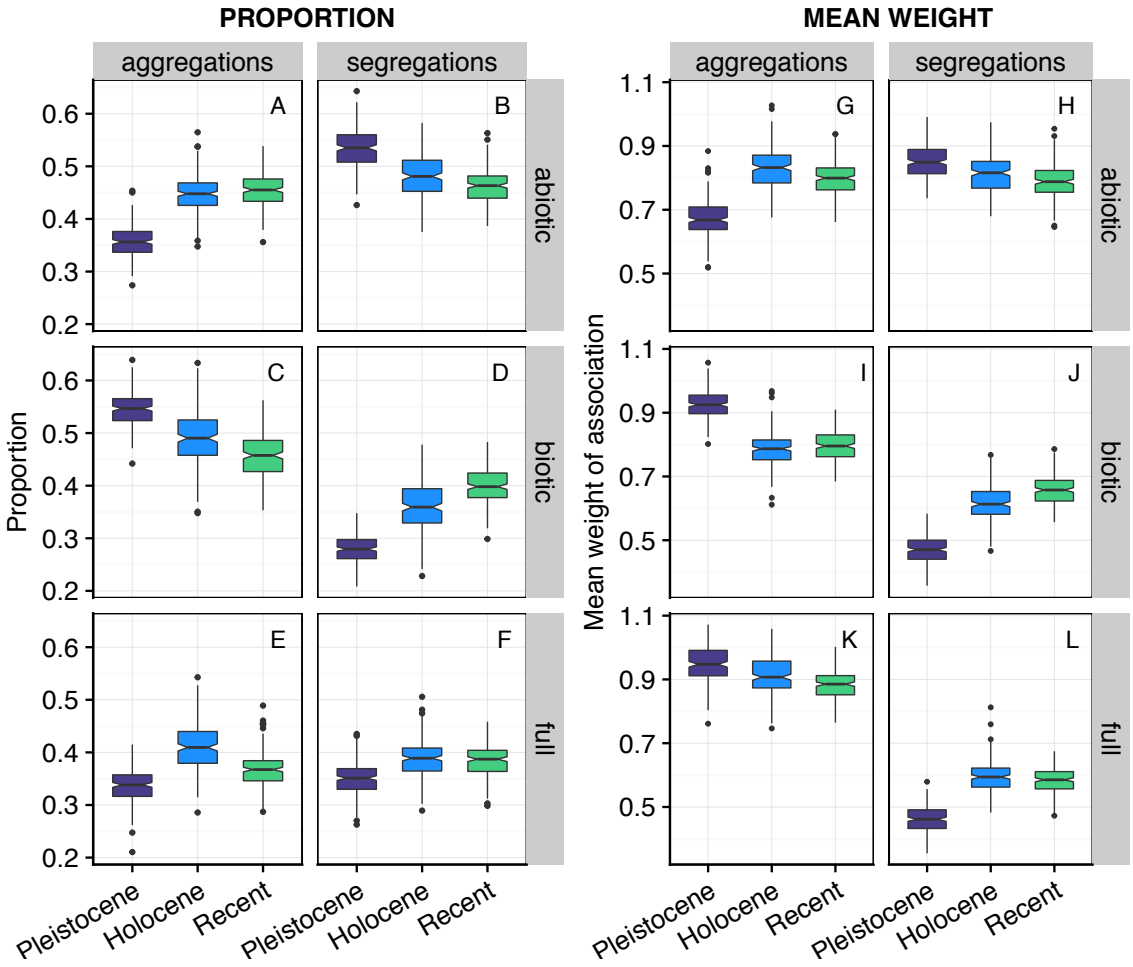

Figure S11.

Results of reduced richness analysis to test for systematic time averaging bias. Proportion (left) and mean weight (right) of aggregations and segregations for abiotic components (top), biotic components (middle), and full associations (bottom) when end-Pleistocene sites with more than 21 species are removed. Boxplots represent variation over subsamples (n= 200). Only pairs with at least 10 sites falling within their mutual potential range are included and all associations are calculated with exactly 10 sites.

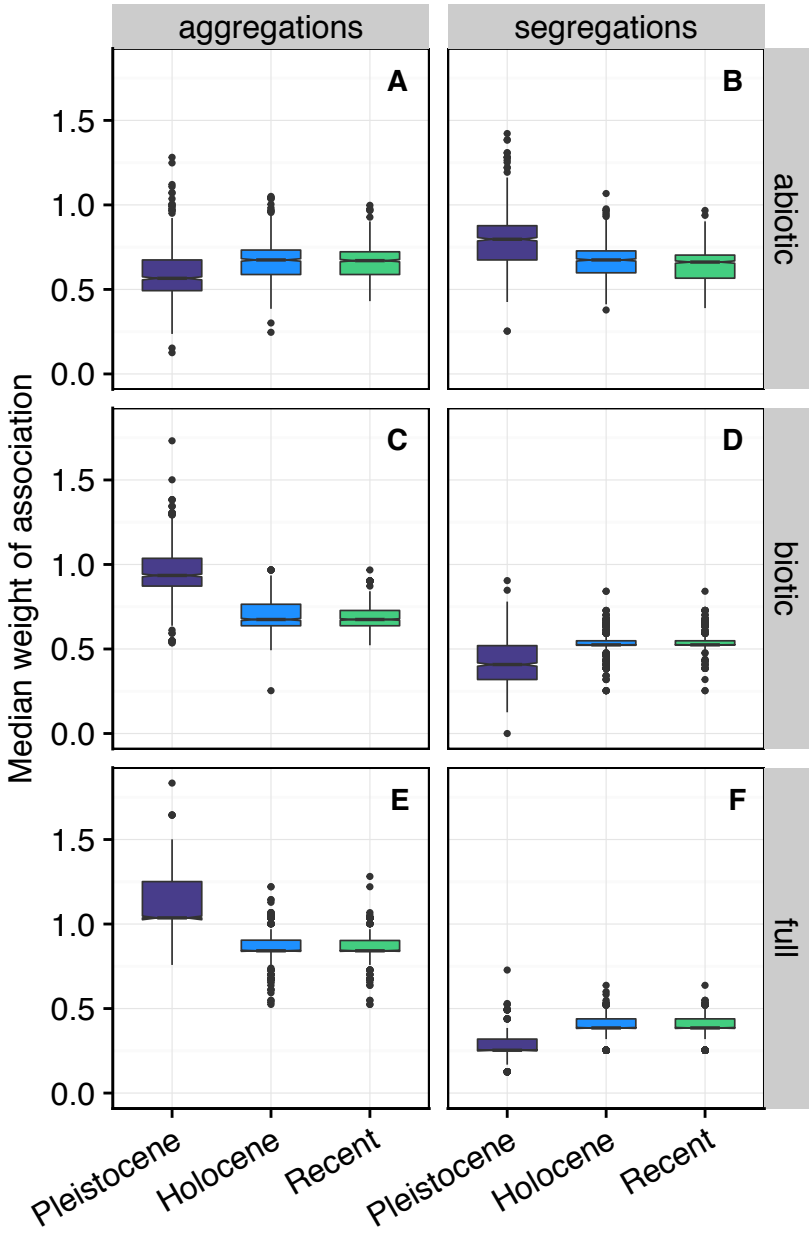

Figure S12.

Median weight of aggregations associations. Abiotic components (A-B), biotic components (C-D), and observed full association (E-F) in each subsample (n = 1000). Only pairs with at least 10 sites falling within their mutual potential range are included.

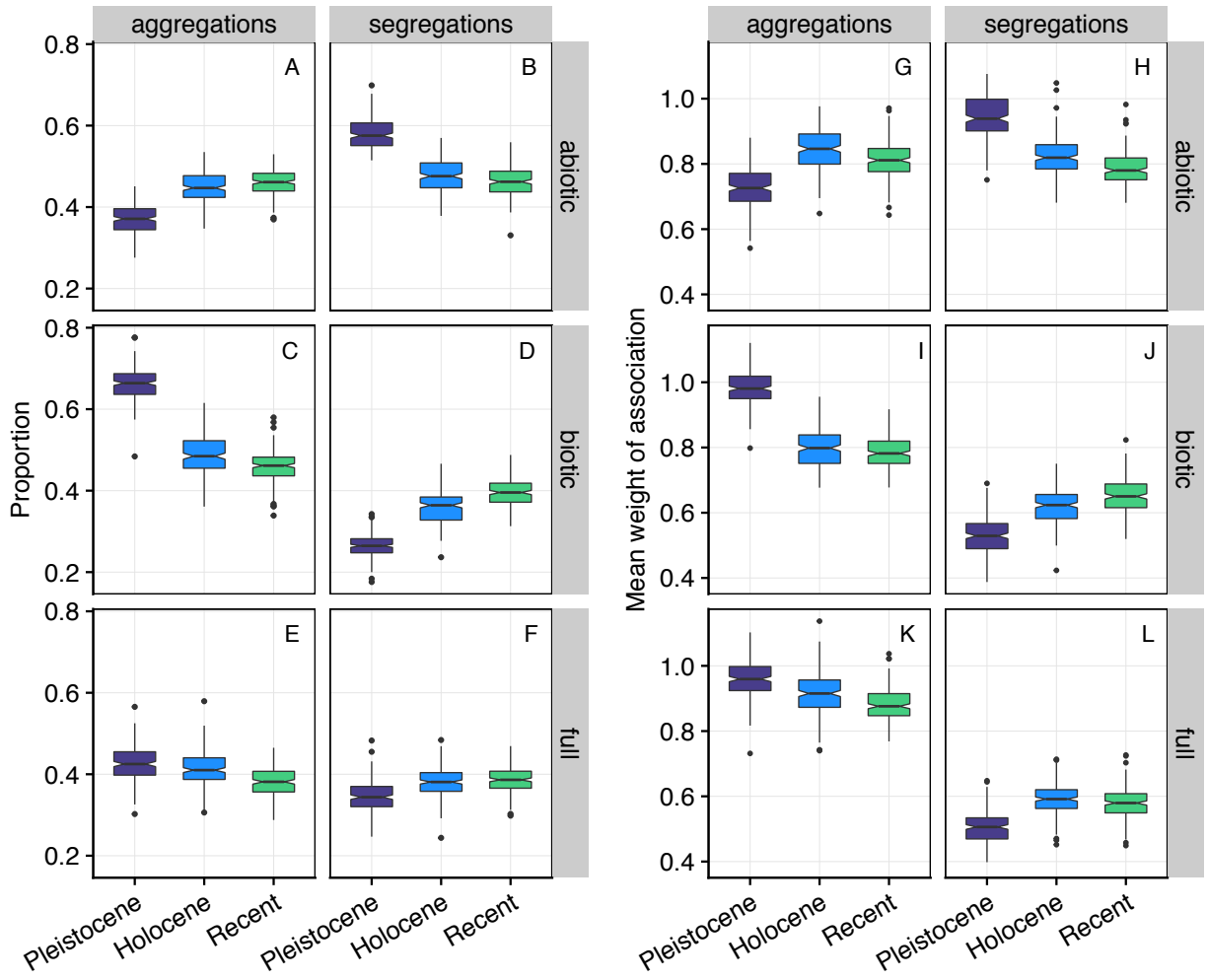

Figure S13.

Results of 4 ka climate averaging to test for systematic dating bias. Proportion (left) and mean weight (right) of aggregations and segregations for abiotic components (top), biotic components (middle), and full associations (bottom) when climates are averaged over 4 ka. Boxplots represent variation over subsamples (n= 200). Only pairs with at least 10 sites falling within their mutual potential range are included and all associations are calculated with exactly 10 sites.

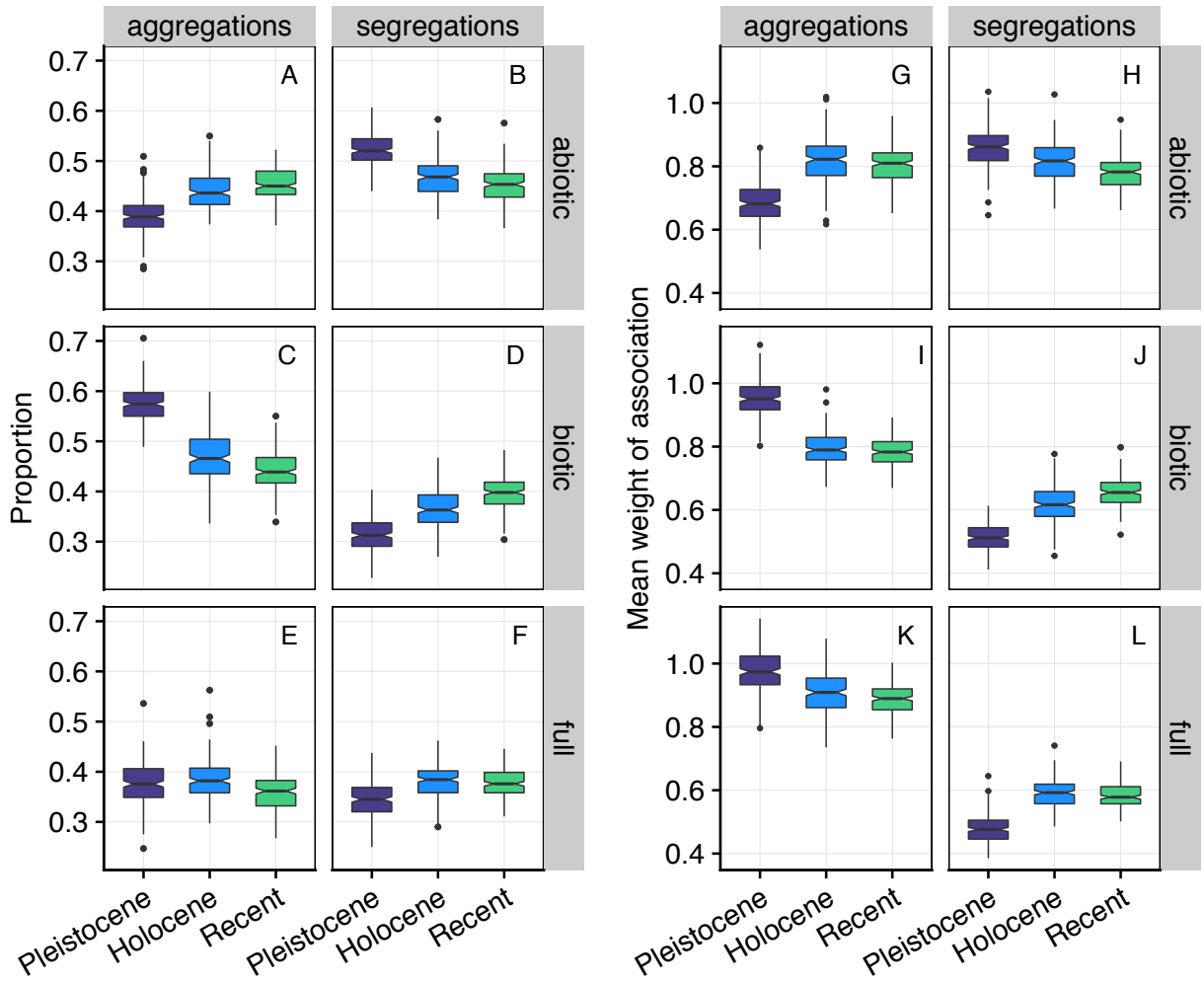

Figure S14.

Results of min/max climate assignments to test for systematic dating bias. Proportion (A-F) and magnitude (G-L) of aggregations and segregations for abiotic components (top), biotic components (middle), and full associations (bottom) when climates are calculated by randomly chosen minimum or maximum calibrated age. Boxplots represent variation over subsamples (n= 200). Only pairs with at least 10 sites falling within their mutual potential range are included.

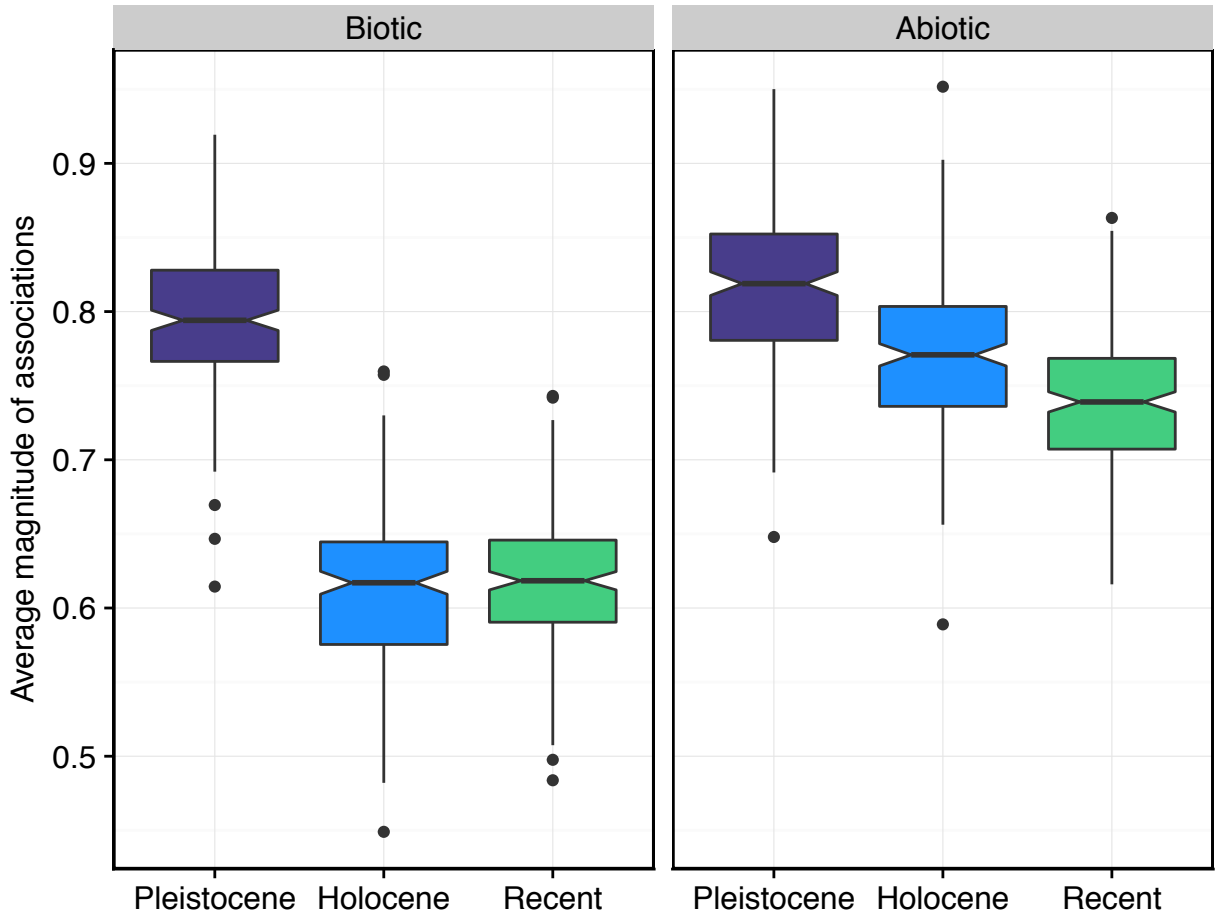

Figure S15.

Abiotic vs Biotic components for 4 ka averaged climates. Average magnitude of biotic and abiotic associations over the three time intervals, broadly representing the relative importance of these two components for overall community assembly patterns, when climates are assigned using 4000-year averages. Boxplots represent the variation among subsamples (n = 200).

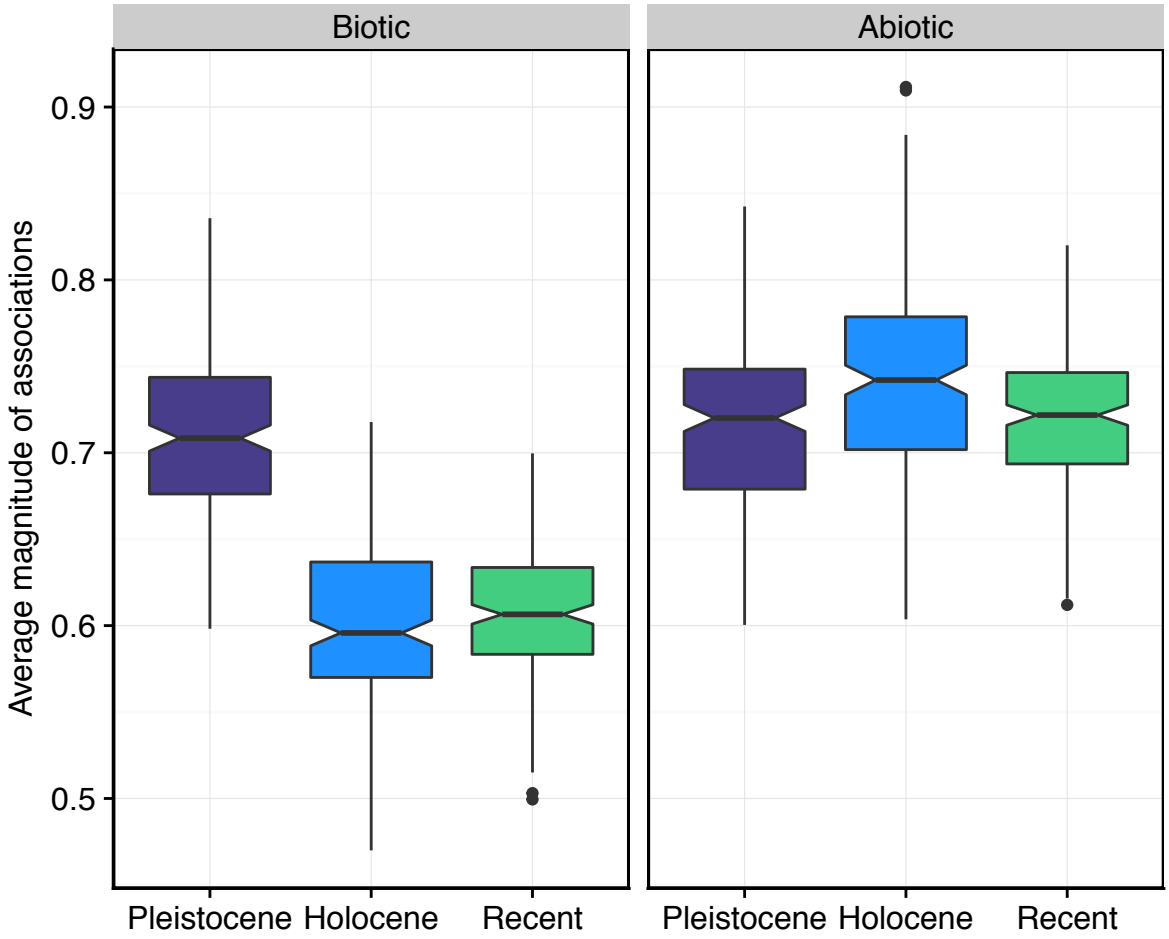

Figure S16.

Abiotic vs Biotic components for min/max climates Average magnitude of biotic and abiotic associations over the three time intervals, broadly representing the relative importance of these two components for overall community assembly patterns, when climates are assigned using 1000-year averages corresponding to minimum or maximum site age (age chosen randomly). Boxplots represent the variation among subsamples (n = 200).

Table S1.

Basic properties of the dataset used in this paper, split by time interval. Note that overlaps in duration between Holocene and end-Pleistocene datasets result from eight Holocene sites with low-precision dates for which their maximum age estimates are older than ~11 ka (the accepted Pleistocene-Holocene boundary)

Epoch	Sites	Species	Matrix fill	Duration (by Max Age)	Occupancy Range	Occupancy Median/Mean
Recent	535	48	0.160	2.0-0 ka	0.600	0.103 / 0.160
Holocene	460	49	0.150	13.1-2 ka	0.573	0.076 / 0.150
End-Pleistocene	72	98	0.0964	21-11 ka	0.444	0.083 / 0.099